Geophys. J. Int. (1993) **114,** 373–391

Seismic attenuation by scattering: theory and numerical results

S. A. Shapiro and G. Kneib

Geophysikalisches Institut, Universität Karlsruhe, Hertzstrasse 16, 76187 *Karlsruhe, Germany*

Accepted 1993 January 14. Received 1993 January 14; in original form 1992 June 9

SUMMARY

Estimates of seismic wave attenuation are strongly affected by scattering. Scattering is an important effect caused by interaction of seismic wavefields with inhomogeneities of hydrocarbon reservoirs, Earth's crust and mantle. In order to study the contribution of scattering to apparent attenuation we consider plane-wave propagation in acoustic 2-D and 3-D inhomogeneous media. Different attenuation estimates result depending on what wavefield function is being averaged during corresponding processing. By wave-theoretical analysis and high-order finite difference modelling in two dimensions we show that scattering attenuation estimates derived from the mean of amplitude spectra and from the mean logarithm of amplitude spectra depend on travel distance. For not too long travel distances, where the coherent part of the wavefield dominates, we give an analytical description of these estimates. In 2-D and 3-D the relations are established between the autocorrelation functions of velocity fluctuations of a random medium and the autocorrelation functions of amplitude and phase fluctuations on a receiver line perpendicular to the general propagation direction of an originally plane wave. For long distances, where the wavefield fluctuates strongly, we show that both mean logarithm of amplitude and logarithm of mean amplitude tend to constants. They differ approximately by a factor two in both scattering regimes. The scattering attenuation coefficient of the meanfield is not dependent on travel distance. We compared our theoretical results with numerical calculations and found excellent agreements. The concept presented clarifies the nature of seismic Q estimations in the presence of scattering and can help to yield statistical earth models from seismic data.

Key words: attenuation, finite differences, random media, scattering, wavefield fluctuations.

INTRODUCTION

For years seismologists have been extensively studying wave propagation in random media. Aki & Chouet (1975) were among the first who predicted small-scale velocity heterogeneities in the earth's crust from the presence of the seismic coda. Aki (1980), Sato (1982), and Wu (1982a,b) started to study theoretical and experimental aspects of seismic waves scattering attenuation. Later Frankel & Clayton (1986) and Jannaud, Adler & Jacquin (1991) used finite difference modelling for a quantitative investigation of the coda decay rate and scattering attenuation. A stochastic approach based on traveltime tomography reveals the Earth's mantle heterogeneity (Gudmundsson, Davies & Clayton 1990; Davies, Gudmundsson & Clayton 1992). Müller, Roth & Korn (1992) analyse traveltimes in random media by finite difference modelling.

Amplitudes and phases of wavefields fluctuate in random media. Averaged wavefields are characterized by attenuation, dispersion and anisotropy (Ishimaru 1978; Rytov, Kravtsov & Tatarskii 1987).

Attenuation of seismic waves is caused by (1) scattering and (2) absorption (intrinsic attenuation). Attenuation by scattering depends on how fast rock parameters vary in space and how large these variations are.

Scattering attenuation and absorption are important parameters for rock characterization. Both can have the same order or one can be stronger than the other dependent on the geology. Attenuation due to scattering can dominate in heterogeneous media.

Scattering attenuation has been theoretically studied in the past (see for example Sato 1982; Wu 1982a,b, 85; Hudson 1990). Theories on wave propagation in random media predict average wavefield quantities for averages over

a statistical ensemble of medium realizations. The following two points are important to relate theoretical results on scattering attenuation and seismological practice.

(1) In practice we are interested in the properties of a specific geological medium and we have to replace ensemble averaging by spatial averaging of a single realization which requires the medium to be ergodic. We will assume that this condition is satisfied.

(2) Different functions of the recorded wavefield differently take into account the wavefield fluctuations caused by scattering. Therefore, different attenuation estimates are obtained dependent on what wavefield function is being averaged (Sato 1982; Wu 1982a). This point is central to this study.

The ensemble-averaged wavefield is described by meanfield theory (Keller 1964). The resultant scattering attenuation is mainly a statistical effect (Sato 1982; Wu 1982a) caused by averaging different realizations of the wavefield having individual phase fluctuations. The real scattering attenuation of seismic wavefields is smaller than that of meanfield. In order to emphasize this fact Wu (1982a) calls the corresponding attenuation coefficient of meanfield 'randomization coefficient'.

Averaging the square of amplitude spectra measures wavefield intensity (Ishimaru 1978; Wu 1985). The intensity of plane waves is attenuated only due to absorption if we can neglect backscattering.

Sato (1982) proposed a formalism to obtain attenuation of wavefield amplitudes averaged after traveltime correction. He assumed a boundary wavelength in the fluctuation spectrum of the inhomogeneities. Fluctuations of wavelengths longer than this value are assumed to cause traveltime fluctuations and smaller wavelengths should cause attenuation. Similar results were obtained by Wu (1982b) under the assumption that seismic amplitudes attenuate only due to scattering in the back halfspace. Both approaches are accepted as a description of seismic pulse-wave attenuation although both of them are based on the heuristic assumptions mentioned above.

In seismology attenuation estimates often are computed from amplitude spectra. In practice one works with the logarithm of the amplitude spectrum (see for example Pujol & Smithson 1991) and obtains attenuation by linear regression. But is linear regression always justified? What kind of estimation does it yield? No theory exists which describes the logarithm of seismic wavefield amplitude spectra in random media and which could answer these questions.

Therefore, a practically relevant theory of seismic body-wave scattering attenuation which is new and a step beyond Sato's and Wu's approaches has to study explicitly the averaged logarithm of the amplitude spectrum of a seismic pulse wavefield. Such a theory should not be strongly restricted by heuristic assumptions.

In this paper we proceed towards this direction. We consider the averaged logarithm of wavefield amplitude spectra in random media. Our restrictions are: (1) plane harmonical wave, (2) acoustic case and constant density, (3) correlation distance of the medium fluctuations is independent on azimuth and of order or larger than the wavelength, (4) medium fluctuations of a constant background are low contrast. Our numerical results show that our theory works satisfactorily for pulse wavefields too.

We compare attenuation estimates based on averaged logarithms of amplitude spectra with scattering attenuation of the averaged amplitude spectra (the order of operations is crucial) and of the meanfield. We consider theoretically all three averages in 2-D and 3-D random media. 2-D theory is necessary to compare with numerical simulation. We describe wavefields in two regimes (regions) of wave propagation: the regions of weak and strong wavefield fluctuations. The region of weak wavefield fluctuations is defined as the region where the coherent part of the wavefield is much larger than the incoherent wavefield. The region of strong fluctuations is defined as the region where the incoherent wavefield component predominates. Our theory is based on the Rytov approximation for the wavefield in the weak fluctuations region. There we obtain the correlation functions of amplitude, phase and traveltime fluctuations. From the amplitude fluctuations we derive scattering attenuation estimates. Assuming that the logarithm of amplitudes is normally distributed, we obtain attenuation estimates in the strong fluctuation region.

We verify our theoretical results by numerical modelling of a pulse wavefield in an acoustic random medium with an exponential correlation function of velocity fluctuations and constant density. Numerical modelling is performed with a high-order finite difference method which has been shown (Kneib & Kerner 1993) to be suitable for wave-propagation simulations in random media.

The paper proceeds as following. First, we present a theory for attenuation estimates obtained from averaged amplitude spectra and the averaged logarithm of amplitude spectra in the weak fluctuation region and then describe the behaviour of these averages in the strong-fluctuation region. Our deviation also yields the autocorrelation functions of amplitude, phase and traveltime in the weak-fluctuation region. Following the theoretical part we describe how we tested our theory by means of finite difference modelling and discuss the results.

THEORY

In our model we consider a plane seismic body wave propagating in a 2-D or 3-D acoustic medium with constant density. The medium has a constant background velocity c_0 and the index of refraction $n(\mathbf{r}) = c_0/c(\mathbf{r})$. The variable n_1 describes the perturbation of the slowness squared $n^2(\mathbf{r}) - 1 \equiv 2n_1$. Under these conditions the wave equation reads

$$\Delta u - \frac{1}{c_0^2}[1 + 2n_1(\mathbf{r})]\frac{\partial^2 u}{\partial t^2} = 0. \tag{1}$$

For $n_1 \ll 1$ one can consider n_1 as a function describing velocity fluctuations: $c(\mathbf{r}) \approx c_0[1 - n_1(\mathbf{r})]$. At a point $\mathbf{r}$ of a random medium we write the wavefield as

$$u(\mathbf{r}, t) = \langle u(\mathbf{r}, t)\rangle + u_f(\mathbf{r}, t), \tag{2}$$

where the angular brackets denote statistical ensemble averaging and an ensemble is defined as a set of the medium realizations. Here t denotes time, $\langle u\rangle$ is the coherent field, and u_f is the fluctuation of u and is called the non-coherent field. The mean of it is $\langle u_f\rangle = 0$. From (2) it follows for the

intensity $I(\mathbf{r}, t) = |u(\mathbf{r}, t)|^2$ that

$$I_t = I_c + I_n, \tag{3}$$

with the total intensity $I_t = \langle I \rangle$, the coherent intensity $I_c = |\langle u \rangle|^2$, and the non-coherent intensity $I_n = \langle |u_f|^2 \rangle$. If we assume that the incident monochromatic plane wave has amplitude unity, we obtain from statistical wave theory for monochromatic waves (Ishimaru 1978) for the coherent intensity

$$I_c = \exp(-2\alpha_{\langle u \rangle} L), \tag{4}$$

where L denotes travel distance through the random medium and $\alpha_{\langle u \rangle} = \alpha_s + \alpha_a$ is the attenuation coefficient of the meanfield. Here α_a is the coefficient of absorption, i.e. intrinsic attenuation, and α_s is the coefficient which describes meanfield attenuation due to scattering. Again we emphasize that Wu (1982a) proposed to call α_s randomization coefficient in order to stress the statistical nature of meanfield attenuation. In the following it is more suitable for us to call α_s scattering coefficient of meanfield in order to emphasize its close connection to the scattering cross-section of the unit volume of the medium and because this convention is widely accepted.

It follows that

$$I_t = \exp(-2\alpha_a' L). \tag{5}$$

Absorption and also partially scattering are taken into account in α_a'. The coefficient α_a' can depend on L and can be obtained by solving the transport equation. If backscattering can be neglected $\alpha_a' \approx \alpha_a$ and if no energy is absorbed total intensity remains constant.

Recording a random field with receiver apertures much larger than $r_c = \max(\lambda, a)$, where λ is the wavelength and a is the correlation length of the medium, yields an approximate measurement of the coherent part of the field because the incoherent part interferes destructively during receiver aperture averaging if the random medium is ergodic, i.e. ensemble and spatial averaging are equivalent. In seismology we usually have point receivers or arrays of point receivers, and either are smaller than the correlation lengths of the random fields. Therefore, the recorded field consists of the coherent part plus most of the non-coherent part and there can be a discrepancy between the behaviour of the recorded field and relation (4).

Seismic attenuation estimates depend on the function $f(u)$ being averaged. We investigate averaged values $\langle f(u) \rangle$ as usual in seismology. Fig. 1 shows sketches of different averaging procedures which have been of interest in scattering attenuation studies in the literature and also for our work. The meanfield $\langle u \rangle$ (Fig. 1, left) is obtained by stacking individual records without any traveltime corrections. The second from the left part of Fig. 1 shows the

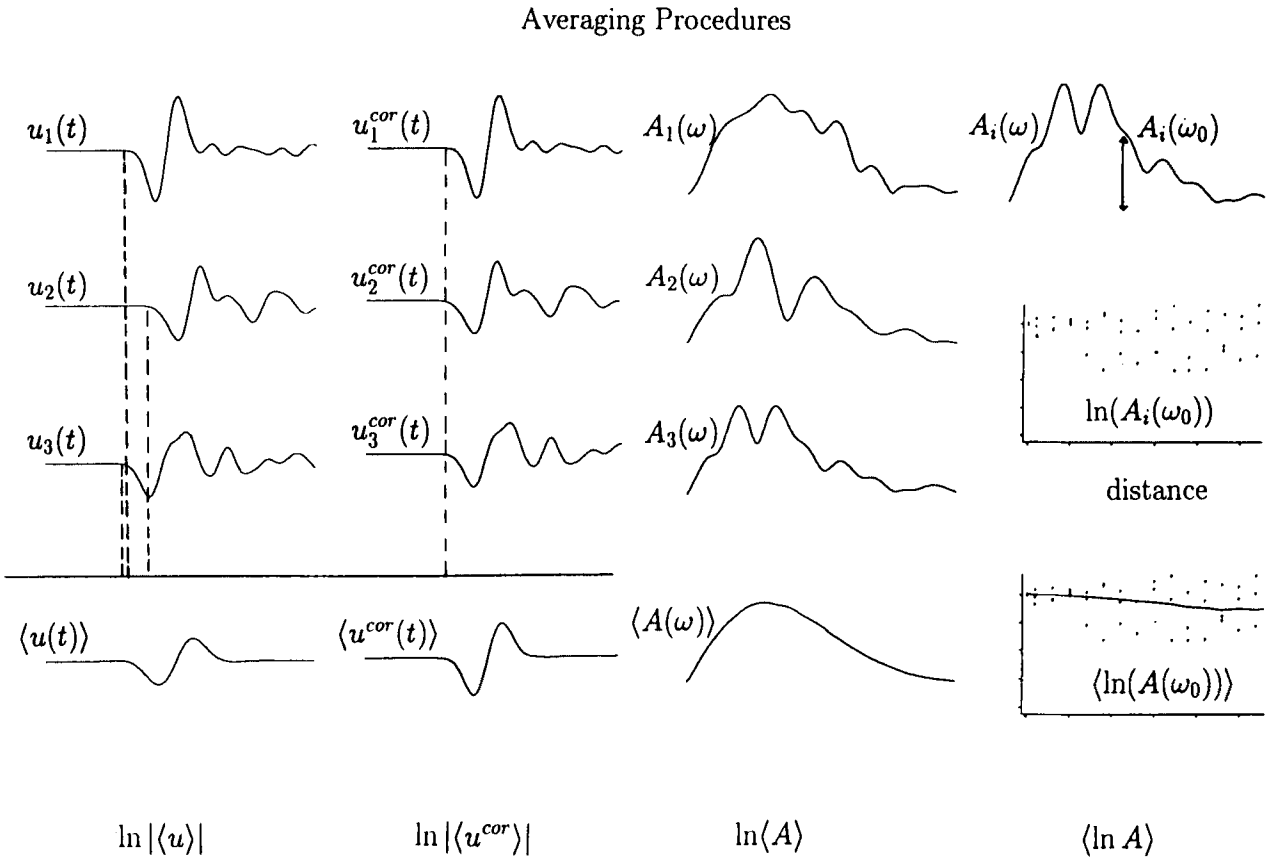

Figure 1. Sketch of averaging procedures. We obtain different scattering-attenuation estimates dependent on what wavefield function we are averaging. The logarithm of meanfield amplitude $\log|\langle u \rangle|$ results from averaging records without phase corrections (left). Averaging records after traveltime corrections (second from left) yields the attenuation estimate described by Sato (1982). Averaging amplitude spectra yields the logarithm of the mean amplitude $\ln\langle A \rangle$ (third from left). The mean logarithm of amplitude $\langle \ln A \rangle$ is the result of averaging only ln amplitudes (right). Scattering-attenuation estimates determine the slope of these logarithms versus travel distance through the random medium.

wavefield averaged after traveltime corrections following Sato (1982). Amplitude decay without influence of traveltime fluctuations can also be measured by stacking amplitude spectra of individual records (Fig. 1, third part from left). Attenuation estimates are then performed by taking the logarithm of the averaged amplitude spectrum. Most relevant for practice is how the cloud of single logarithms of amplitude spectra computed from individual records depends on distance (Fig. 1, right). Formally, the behaviour of the centre of mass of this cloud at each distance can be described as a dependence of the averaged logarithm of amplitude spectra on distance. The two last procedures differ only by what is made first: averaging (stacking) or taking the logarithm.

Usually it is assumed that both the dependence of the logarithm of the averaged amplitude spectrum $\ln\langle A\rangle$ and the average of logarithms of amplitude spectra $\langle \ln A\rangle$ on distance can be fitted by a straight line. The underlying assumption here is that the corresponding attenuation estimates which are determined from the slope of the fitted line are independent on travel distance. Moreover, usually one does not consider a difference between these two values.

In the following paragraphs we shall study the latter two averages and we shall compare them with the behaviour of the logarithm of the amplitude spectrum of the meanfield. We derive approximate formulae that relate $\langle \ln A\rangle$, $\ln\langle A\rangle$, and $\ln|\langle u\rangle|$ to travel distance, frequency and medium statistics. This yields global attenuation estimates which can be written as

$$\alpha_{\ln A}^{\mathrm{glob}} = -\langle \ln A\rangle/L; \qquad \alpha_{A}^{\mathrm{glob}} = -\ln\langle A\rangle/L.$$
$$\alpha_{\langle u\rangle}^{\mathrm{glob}} = -\ln|\langle u\rangle|/L. \tag{6}$$

The local estimates of the attenuation can be written as

$$\alpha_{\ln A}^{\mathrm{loc}} = -\frac{\partial}{\partial L}\langle \ln A\rangle; \qquad \alpha_{A}^{\mathrm{loc}} = -\frac{\partial}{\partial L}\ln\langle A\rangle;$$
$$\alpha_{\langle u\rangle}^{\mathrm{loc}} = -\frac{\partial}{\partial L}\ln|\langle u\rangle|. \tag{7}$$

It will be clear from the following that only for the meanfield these estimates ($\alpha_{\langle u\rangle}^{\mathrm{glob}}$ and $\alpha_{\langle u\rangle}^{\mathrm{loc}}$) are the same.

As a measure of wavefield fluctuations we introduce the parameter θ defined as ratio of incoherent field to coherent field: $\theta \equiv |u_{\mathrm{f}}|/|\langle u\rangle|$. In a random medium without energy dissipation, the coherent field and its intensity attenuate due to the energy transfer from $\langle u\rangle$ to u_{f}. Therefore, the region of weak wavefield fluctuations is limited to small propagation distances where $\theta \ll 1$. For large L we have $\theta \gg 1$ and this part of the medium is the region of strong wavefield fluctuations. The transfer from the weak fluctuation region to the strong fluctuation region occurs where θ has order unity.

Weak fluctuation region

In this paragraph we derive $\langle \ln A\rangle$, $\ln\langle A\rangle$, $\alpha_{\ln A}^{\mathrm{glob}}$, $\alpha_{A}^{\mathrm{glob}}$, $\alpha_{\ln A}^{\mathrm{loc}}$ and $\alpha_{A}^{\mathrm{loc}}$ in the region of weak wavefield fluctuations.

The intensity I of the recorded field is—apart from constants—the square of the field amplitude

$$I \equiv A^2 = I_{\mathrm{t}} + \epsilon, \tag{8}$$

where ϵ is the fluctuation of I and $\langle\epsilon\rangle = 0$. From (2) we get

$$\epsilon = \langle u^*\rangle u_{\mathrm{f}} + \langle u\rangle u_{\mathrm{f}}^* + O(\theta^2) I_{\mathrm{c}}. \tag{9}$$

One can see that $\epsilon = O(\theta) I_{\mathrm{c}}$. Taylor expansions of A and $\ln A$ yield by using (8):

$$\langle \ln A\rangle = 0.5 \ln I_{\mathrm{t}} - 0.25\langle\epsilon^2\rangle/I_{\mathrm{t}}^2 + O(\theta^3), \tag{10}$$

and

$$\ln\langle A\rangle = 0.5 \ln I_{\mathrm{t}} - 0.125\langle\epsilon\rangle^2/I_{\mathrm{t}}^2 + O(\theta^3). \tag{11}$$

Eq. (8) gives for $\langle\epsilon\rangle^2$

$$m^2 \equiv \frac{\langle\epsilon^2\rangle}{I_{\mathrm{t}}^2} = \frac{\langle I^2\rangle - \langle I\rangle^2}{\langle I\rangle^2}. \tag{12}$$

Here m^2 is the scintillation index (Ishimaru 1978) which describes the variance of the intensity. Let us now write u as

$$u = u_0 \exp(\psi) = u_0 \exp(\chi + is). \tag{13}$$

Eq. (13) is often called Rytov transformation. χ and s are random rational functions which are called the level of amplitude and phase fluctuation respectively. Using this transformation we obtain

$$\chi = \ln A - \ln|u_0|. \tag{14}$$

Now using the Taylor expansion of $(\ln A)^2$ and (10) obtain the variance of the amplitude level:

$$\sigma_\chi^2 \equiv \langle(\chi - \langle\chi\rangle)^2\rangle = 0.25\langle\epsilon^2\rangle/I_{\mathrm{t}}^2 + O(\theta^3). \tag{15}$$

Therefore, instead of (10) and (11) we have

$$\langle \ln A\rangle = 0.5 \ln I_{\mathrm{t}} - \sigma_\chi^2 + O(\theta^3), \tag{16}$$

and

$$\ln\langle A\rangle = 0.5 \ln I_{\mathrm{t}} - 0.5\sigma_\chi^2 + O(\theta^3). \tag{17}$$

Let us emphasize that these two relations have been obtained here for a general case, namely a harmonic plane wave in the weak fluctuation region, and without any restrictions of the probability density of χ. In case of spherical waves these relations will be valid too. It is straightforward that

$$\ln\langle A\rangle - \langle \ln A\rangle = 0.5\sigma_\chi^2 + O(\theta^3). \tag{18}$$

This relation is interesting because it yields an amplitude measure which is independent of the total intensity. This difference allows us to study statistical properties of the medium without any theoretical model of the behaviour of I_{t}. This is important because the latter is difficult to derive for spherical waves if the inhomogeneities are not very small.

The second remark we would like to make is the following. In random media χ usually has a normal distribution. Physically this means that the amplitude results from a wavefield which crossed statistically independent parts of the random medium (Rytov *et al.* 1987). Making use of the normal distribution of χ (12) and (13) yields

$$m^2 = \exp[4\sigma_\chi^2] - 1. \tag{19}$$

In the weak fluctuation region σ_χ^2 is small and Taylor expansion yields:

$$m^2 \approx 4\sigma_\chi^2. \tag{20}$$

This connection between the scintillation index and the variance of the amplitude level again leads to (16) and (17) from (10) and (11). A similar way of obtaining relations analogous to (16) and (17) was used by Rytov *et al.* (1987) using the assumption of normal distributed χ.

We continue now in our derivation. If we neglect backscattering (i.e. I_t is a constant which we suppose to be 1) and take into account that $\sigma_\chi^2 = O(\theta^2)$ we can expect in the weak fluctuation region

$$\langle \ln A \rangle \approx -\sigma_\chi^2, \tag{21}$$

and

$$\ln \langle A \rangle \approx -0.5\sigma_\chi^2. \tag{22}$$

Now the problem of relating scattering attenuation to $\langle \ln A \rangle$ and $\ln \langle A \rangle$ is reduced to relating scattering attenuation to the variance of the amplitude level σ_χ^2. Furthermore, we can expect that $\alpha_{\ln A} \approx 2\alpha_A$ and it is sufficient to study $\langle \ln A \rangle$.

In the Appendix 1 we derive the amplitude level and phase fluctuation correlation functions for 2-D isotropic random media with the correlation distance of the order or larger than the wavelength. In the weak fluctuation region the Rytov approximation can be used for the derivation. These correlation functions read (see also A1–10 and A1–11):

$$B_\chi(\Delta z) = 2k^2\pi L \int_0^\infty \cos(\xi\,\Delta z) \times \left(1 - \frac{\sin(\xi^2 L/k)}{\xi^2 L/k}\right) \Phi_n^{2\text{-D}}(\xi)\, d\xi, \tag{23}$$

$$B_s(\Delta z) = 2k^2\pi L \int_0^\infty \cos(\xi\,\Delta z) \times \left(1 + \frac{\sin(\xi^2 L/k)}{\xi^2 L/k}\right) \Phi_n^{2\text{-D}}(\xi)\, d\xi, \tag{24}$$

where $\Phi_n^{2\text{-D}}$ is the 2-D Fourier transform of the corelation function of the index n_1 (or velocity) given by (A2–10). These relations are slightly different in 3-D (Ishimaru 1978):

$$B_\chi(\Delta z) = 2k^2\pi^2 L \int_0^\infty \xi J_0(\xi\,\Delta z) \times \left(1 - \frac{\sin(\xi^2 L/k)}{\xi^2 L/k}\right) \Phi_n^{3\text{-D}}(\xi)\, d\xi \tag{25}$$

$$B_s(\Delta z) = 2k^2\pi^2 L \int_0^\infty \xi J_0(\xi\,\Delta z) \times \left(1 + \frac{\sin(\xi^2 L/k)}{\xi^2 L/k}\right) \Phi_n^{3\text{-D}}(\xi)\, d\xi, \tag{26}$$

where $\Phi_n^{3\text{-D}}$ is the 3-D fluctuation spectrum given by (A2–13).

Before proceeding let us make the following note about the phase fluctuations correlation functions. As is shown by Müller *et al* (1992) and Gudmundsson *et al.* (1990) the statistics of traveltime fluctuations can be very useful for an inversion of medium statistics. In these studies the geometrical optics approximation has been used. The relations (24) and (26) are more general because they are valid not only for very short wavelengths but for wavelengths up to the order of a and contain the geometrical optics approximation as a special case. In the geometrical optics approximation it is assumed that $L \ll a^2/\lambda$ ($\sqrt{\lambda L}$ is the Fresnel zone). The medium fluctuation spectrum Φ_n differs from 0 noticeably only for $\xi \lesssim 2\pi/a \ll 2\pi/\sqrt{\lambda L}$. This means that the factor $\left(1 + \frac{\sin(\xi^2 L/k)}{\xi^2 L/k}\right)$ in the integrands of (24) and (26) is approximately equal 2. Substituting then relations (A2–10) and (A2–13), integration over ξ, and taking into account that phase fluctuations are the fluctuations of traveltimes multiplied by angular frequency yield exactly the relation (4) from Müller *et al.* (1992) for the autocorrelation function of the traveltime fluctuations.

Here we are interested in the variances σ_χ^2 and σ_s^2. Taking the corresponding correlation functions at zero lag yields these variances. The formulae for variances are very similar to (23), (24), (25) and (26) with the only difference that in the integrands the factors with cos in the 2-D case and with Bessel functions in the 3-D case are equal unity. From that and (A2–16) and (A2–17) it is straightforward to obtain

$$\sigma_\chi^2 + \sigma_s^2 = 2\alpha_s L. \tag{27}$$

This relation shows that attenuation of the mean field is not only caused by phase fluctuations but also due to amplitude fluctuations. Relation (27) can be obtained directly from (13) by using the assumption that χ and s are normal distributed.

The value $\langle \ln A \rangle$ depends on σ_χ^2 only and, therefore, its behaviour with L is more complicated than a simple proportionality:

$$\langle \ln A \rangle_{2\text{-D}} \approx -\sigma_\chi^2 \approx -2k^2\pi L \times \int_0^\infty \left(1 - \frac{\sin(\xi^2 L/k)}{\xi^2 L/k}\right) \Phi_n^{2\text{-D}}(\xi)\, d\xi. \tag{28}$$

Let us give a more detailed analysis of (28). First note that this relation is slightly different in 3-D problems:

$$\langle \ln A \rangle_{3\text{-D}} \approx -\sigma_\chi^2 \approx -2k^2\pi^2 L \times \int_0^\infty \xi \left(1 - \frac{\sin(\xi^2 L/k)}{\xi^2 L/k}\right) \Phi_n^{3\text{-D}}(\xi)\, d\xi. \tag{29}$$

If $L \ll a^2/\lambda$ (i.e. we apply the geometrical optics approximation) we can use the Taylor expansion of $\sin(\xi^2 L/k)$ for small arguments. Therefore,

$$\langle \ln A \rangle_{2\text{-D}} \approx -\frac{\pi L^3}{3} \int_0^\infty \xi^4 \Phi_n^{2\text{-D}}(\xi)\, d\xi, \tag{30}$$

$$\langle \ln A \rangle_{3\text{-D}} \approx -\frac{\pi^2 L^3}{3} \int_0^\infty \xi^5 \Phi_n^{3\text{-D}}(\xi)\, d\xi. \tag{31}$$

In the case $L \gg a^2/\lambda$ we have $2\pi/a \gg 2\pi/\sqrt{L\lambda}$ and the main contribution in the integrals (28) and (29) stems from $\xi > 2\pi/\sqrt{\lambda L}$. This means that

$$\langle \ln A \rangle_{2\text{-D}} \approx -2\pi k^2 L \int_0^\infty \Phi_n^{2\text{-D}}(\xi)\, d\xi, \tag{32}$$

$$\langle \ln A \rangle_{3\text{-D}} \approx -2\pi^2 k^2 L \int_0^\infty \xi \Phi_n^{3\text{-D}}(\xi)\, d\xi. \tag{33}$$

As is shown in Appendix 2, the integrals in (32) and (33) are proportional to the scattering cross-sections of unit volumes

of 2-D and 3-D media respectively, for $a/\lambda \gtrsim 1$. i.e. for $L \gg a^2/\lambda$ we have

$$\langle \ln A \rangle \approx -\alpha_s L. \tag{34}$$

This result has already been obtained by Fayzullin & Shapiro (1988).

If the index n_1 has an isotropic exponential correlation function (see Appendix) and a variance σ_n^2 then the fluctuation spectrum of the medium is

$$\Phi_n^{2\text{-D}}(\xi) = \frac{\sigma_n^2 a^2}{[1+(\xi a)^2]^{3/2}}, \tag{35}$$

and the amplitude level variance can be computed explicitly from (28) which yields

$$\langle \ln A \rangle_{2\text{-D}} \approx -L\sigma_n^2 ak^2 \left\{ 1 + \frac{\pi}{2}[J_1(b)\cos b + Y_1(b)\sin b] \right\}. \tag{36}$$

Here $b = L/(2a^2k)$ and J_1 and Y_1 are the Bessel functions of the first and second kind. The scattering attenuation estimations obtained from $\langle \ln A \rangle$ and from $\ln \langle A \rangle$ depend on travel-distance L because L appears in the argument of the Bessel and trigonometric functions.

The global scattering attenuation estimates obtained in 2-D and 3-D from $\langle \ln A \rangle$ and described by (6) are the same as (28) and (29) except for a factor $-L$ before the integrals. With (A2–16) and (A2–17) we obtain:

$$\alpha_{\ln A}^{\text{glob}} \approx \alpha_s - 2k^2\pi \int_0^\infty \frac{\sin(\xi^2 L/k)}{\xi^2 L/k} \Phi_n^{2\text{-D}}(\xi)\, d\xi \tag{37}$$

in 2-D and

$$\alpha_{\ln A}^{\text{glob}} \approx \alpha_s - 2k^2\pi^2 \int_0^\infty \xi \frac{\sin(\xi^2 L/k)}{\xi^2 L/k} \Phi_n^{3\text{-D}}(\xi)\, d\xi \tag{38}$$

in 3-D.

The local attenuation estimates can be obtained by (7), (28) and (29) and taking into account (A2–16) and (A2–17):

$$\alpha_{\langle \ln A \rangle}^{\text{loc}} \approx \alpha_s - 2k^2\pi \int_0^\infty \cos(\xi^2 L/k) \Phi_n^{2\text{-D}}(\xi)\, d\xi \tag{39}$$

in 2-D and

$$\alpha_{\langle \ln A \rangle}^{\text{loc}} \approx \alpha_s - 2k^2\pi^2 \int_0^\infty \xi \cos(\xi^2 L/k) \Phi_n^{3\text{-D}}(\xi)\, d\xi \tag{40}$$

in 3-D.

These four relations explicitly show the deviations of the global and local attenuation estimates from the coefficient of scattering attenuation of the mean field α_s. The deviations depend non-linearly on the travel distance and they are described by the Fourier-type integrals of the medium fluctuation spectrum. This means that they can be used for an inversion. The difference between local and global estimations is obvious, but for large travel distances, both global and local estimations asymptotically tend to the scattering coefficient of the meanfield (at least for quadratically integrable spectra Φ_n). As attenuation estimates obtained by Sato (1982) or Wu (1982b) estimates based on $\langle \ln A \rangle$ are also smaller than α_s. But in contrast to their results these estimates depend on travel distance.

In Fig. 2 we plot the travel-distance dependence of three attenuation parameters calculated for a 3-D medium with

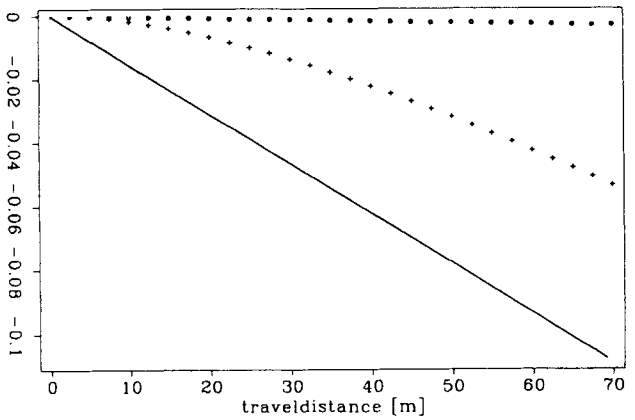

Figure 2. The travel distance dependence of (1) the logarithm of the meanfield amplitude (solid line); (2) the logarithm of the wavefield amplitude calculated in the approximation of Wu [relation (17), 1982b; dotted line], and (3) the averaged logarithm of the amplitudes [relation (29) from this paper, denoted by crosses]. The curves have been calculated for a 3-D medium with exponential correlation function, a correlation distance $a = 20$ m, with an average velocity of 3000 m s^{-1}, a standard deviation of the velocity fluctuations of 90 m s^{-1}, and a frequency of 100 Hz.

exponential correlation function. For this particular example we chose $a = 20$ m, an average velocity of 3000 m s^{-1}, a standard deviation of the velocity fluctuations of 90 m s^{-1} and a frequency of 100 Hz. The solid line shows the logarithm of the meanfield amplitude $\left[\alpha_s = B_n(0)\frac{4k^4a^3}{1+4k^2a^2}\right]$. The dotted line shows the logarithm of the wavefield amplitude calculated in Wu's approximation [relation (17), Wu 1982b]. The crosses denote the averaged logarithm of the amplitudes (29). For small travel distances the latter curve is close to the dotted line but with increasing travel distance it deviates more and more to the solid line. The physical interpretation is: at short travel distances meanfield attenuates mainly because of arrival-time fluctuations of individual records. Both estimates corresponding to the dotted and crossed lines are independent of these fluctuations. With increasing travel-distance, amplitude fluctuations play an increasing role in meanfield attenuation. The crossed line describes a pure amplitude fluctuations effect. This is why the crossed line deviates to the solid line. Therefore, Wu's approximation (and similarly Sato's traveltime corrected estimation) underestimate the influence of amplitude fluctuations on scattering attenuation estimates.

On the other hand, Fig. 2 shows also that applying the linear regression to the travel-distance dependence of the logarithm of amplitude leads to misinterpretations. Let us finally note that the estimations obtained from $\ln \langle A \rangle$ are two times smaller than those obtained from $\langle \ln A \rangle$.

Strong fluctuation region

Consider now the wavefield behaviour in the strong fluctuation region ($\theta \gg 1$) and remember the exponential representation of the wavefield (13). If the intensity of the incident field is unity this representation will give

$$\langle \ln A \rangle = \langle \chi \rangle, \tag{41}$$

and on the other hand

$$\langle e^{2\chi} \rangle = I_t. \tag{42}$$

Let us make the assumption that the amplitude function χ has a normal distribution. This is generally true in the weak fluctuation region (Rytov *et al.* 1987; Ishimaru 1987) and recalling the central limit theorem it should be approximately correct in the strong fluctuation region. Therefore,

$$\langle e^{2\chi} \rangle = e^{2\langle \chi \rangle + 2\sigma_\chi^2}, \tag{43}$$

which leads to

$$2\langle \chi \rangle = \ln I_t - 2\sigma_\chi^2. \tag{44}$$

These two relations yield

$$\langle \ln A \rangle = 0.5 \ln I_t - \sigma_\chi^2, \tag{45}$$

and

$$\ln \langle A \rangle = 0.5 \ln I_t - 0.5\sigma_\chi^2. \tag{46}$$

We have obtained relations (16) and (17) again. Provided χ is normally distributed these relations are exact.

Fluctuations of the amplitude level reach a state of saturation in the strong fluctuation region. In the limit $L \to \infty$ the variance of intensity and therefore the scintillation index $m \to 1$ (Rytov *et al.* 1987; Ishimaru 1978). From (19) it follows that $\sigma_\chi^2 = \text{const} = 0.25 \ln (2) \approx 0.173$. Provided backscattering can be neglected, i.e. $I_t \approx 1$, both values $\langle \ln A \rangle$ and $\ln \langle A \rangle$ will tend to constants -0.173 and -0.087 respectively. One important consequence is that in the strong fluctuation region the global estimates of attenuation will decrease as $1/L$ if $L \to \infty$ and the local estimates will tend to zero, too. The resulting bias in the attenuation estimate can lead to serious misinterpretations.

NUMERICAL EXPERIMENT

We computed synthetic shot records of the plane wave that propagated through a 2-D acoustic random medium with constant density. The aim of the modelling is to demonstrate the validity of the main theoretical conclusions about the behaviour of $\langle u \rangle$ (Appendix 2), $\ln \langle A \rangle$, and $\langle \ln A \rangle$ and their importance for attenuation estimation in seismology.

Our numerical experiment involved three steps: (1) producing a random medium with specified statistical parameters, (2) computing shot records with finite differences, and (3) extracting attenuation from the synthetic data and comparing with the presented theoretical results.

Most common random media models are based on 2-D random fields of normal distributed parameters with Gaussian, exponential and von Karman autocorrelation functions. These simple models are useful not only for investigations of wave propagation in the lithosphere (Frankel & Clayton 1986) but also in seismic exploration (Gibson & Levander 1990).

The velocity fluctuation of our random models is characterized by the Gaussian distribution function of the P-wave velocity with the mean $3000\,\text{m s}^{-1}$ and relative standard deviation 3 per cent and by the isotropic exponential autocorrelation function with the correlation length $a = 20$ m. Density is constant. The model used in our wave propagation simulation (Fig. 3, bottom) contains

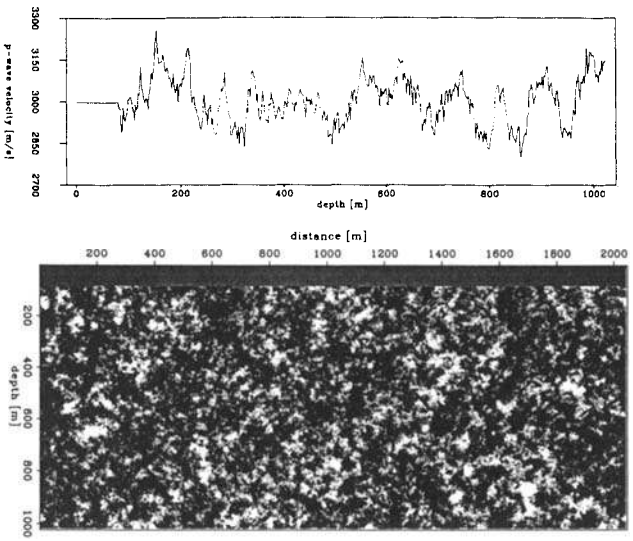

Figure 3. Random model used for the numerical experiment. Bottom: a homogeneous zone is followed by a random medium with an isotropic exponential distribution function and a correlation length of 20 m. A vertical trace through the medium illustrates how fast the medium fluctuates (top).

1000×400 grid points with a grid interval of 2 m. A vertical trace through the medium (Fig. 3, top) illustrates how fast velocity fluctuates.

We let a plane wave propagate through the random medium and register the wavefield at many geophones for each of several propagation distances (Fig. 4). The subsequent processing was then performed based on the common travel-distance gathers. In order to get good averaging, the lengths of the receiver lines have to be much larger than $\max(a, \lambda_{max})$. We choose the distances between geophones along the receiver lines and the distances between receiver lines so that they are of order

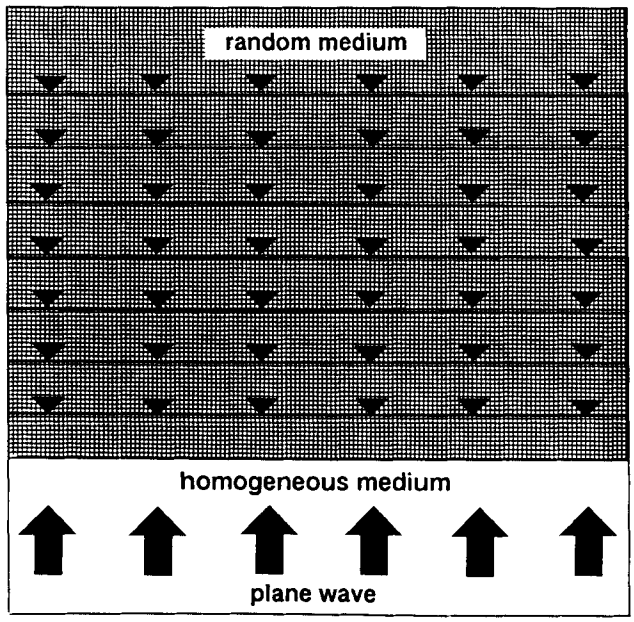

Figure 4. Experimental set-up for the wavefield simulations. A plane wave enters a random medium and the scattered field is registered at several receivers and propagation distances.

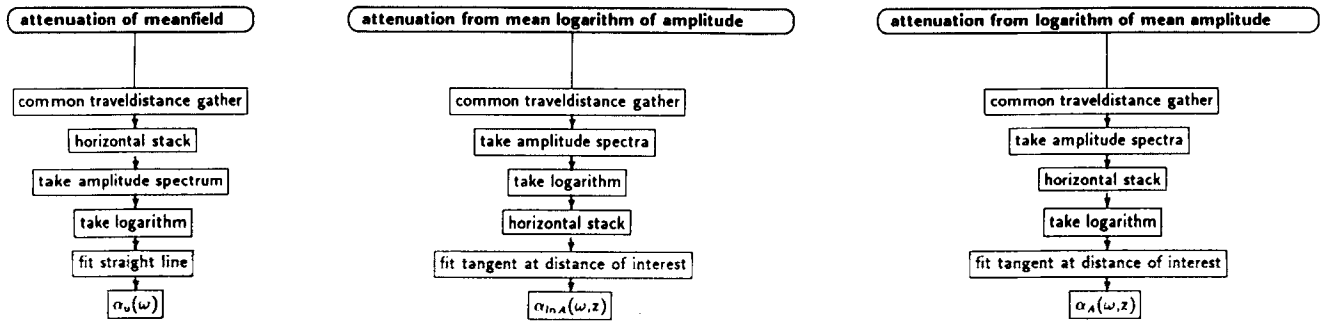

Figure 5. Processing sequences to compute $\ln|\langle u\rangle|$, $\ln\langle A\rangle$, and $\langle\ln A\rangle$. Each yields a different scattering-attenuation estimate.

$\max(a, \lambda_{\max})$. This avoids processing of many statistically dependent measurements. To avoid artificial damping of the plane wave with traveltime we apply periodic boundary conditions at the left and right side of the grid. Seismic waves are absorbed at the top and bottom boundaries parallel to the originally plane wave. To make sure that the results are not biased by the periodic boundaries we exclude the outermost traces from our analysis. The source is located in a small homogeneous region with the constant replacement velocity c_0 of the random medium. The source wavelet is the first derivative of a Gaussian with a dominant frequency of 100 Hz and a maximum frequency of about 300 Hz. Given the mean velocity, the dominant wavelength is 30 m. Wave propagation in this regime can be characterized by the dimensionless wavenumber $ka \approx 4.2$ where $k = \dfrac{2\pi}{\lambda_{\text{dominant}}}$.

Analysis of numerical dispersion and attenuation caused by the our finite difference scheme shows that eighth-order accuracy in space and fourth-order accuracy in time yield sufficient accuracy in the wavefield modelled (Kneib & Kerner 1993). We validated this by repeating our attenuation estimation procedure for models with identical grid sizes as in the random medium simulations but with the constant slowness $1/c_0$. The results show that the logarithm of the meanfield spectrum deviates only slightly from the expectation value of zero with log values always below 0.1 per cent of the equivalent random medium experiment.

Fig. 5 shows the simple processing sequence to obtain meanfield attenuation (left), the logarithm of the mean amplitude (centre), and the mean logarithm of amplitude spectra (right). The only difference is the order of operations. The meanfield theory requires to stack immediately after common travel-distance gathers could be collected. The travel-distance dependence of the logarithm of the meanfield amplitude spectrum for a given frequency can then be fitted by a straight line whose slope is the scattering coefficient α_s. Computing amplitude spectra for each trace in the common travel distance gathers, stacking and taking the logarithm for given frequency yields the logarithm of mean amplitude $\ln\langle A\rangle$. If we take amplitude spectra of each trace, take the logarithm of the spectra, and stack afterwards, we shall obtain the mean logarithm of amplitude spectra $\langle\ln A\rangle$.

The numerical modelling was performed in the time domain. We studied the propagation of the pulse which had the form of the first time derivative of the Gaussian curve. The theoretical results were obtained for a harmonic wavefield. Therefore, in order to compare numerical and theoretical results we have to perform the Fourier analysis of the complete traces without windowing. Putting a short window around the main coherent arrival would exclude the fluctuations contained in the coda. However, studying statistical moments of harmonic wavefields requires complete traces because scattered energy from the coda also contributes to these moments. Of course, the exclusive processing of 'direct arrivals' requires windowing and the theory should be extended accordingly. In the discussion section we shall consider the problem of windowing and demonstrate at least the qualitative validity of the presented theory for the 'direct arrivals', too.

Results

Fig. 6 shows shot records registered at different propagation distances through a random medium. The left record corresponds to the region of weak wavefield fluctuations and has been obtained after the wavefield travelled 20 m through the random medium. The strong fluctuating wavefield passed 620 m through the random medium and is shown on Fig. 6, right. Both wavefields have been bandpassed with a centre frequency of 160 Hz. As a result $\theta \approx 0.3$, resp $\theta \approx 3.3$. for the centre frequency. This corresponds to $\alpha_{\langle u\rangle}L = 0.04$,

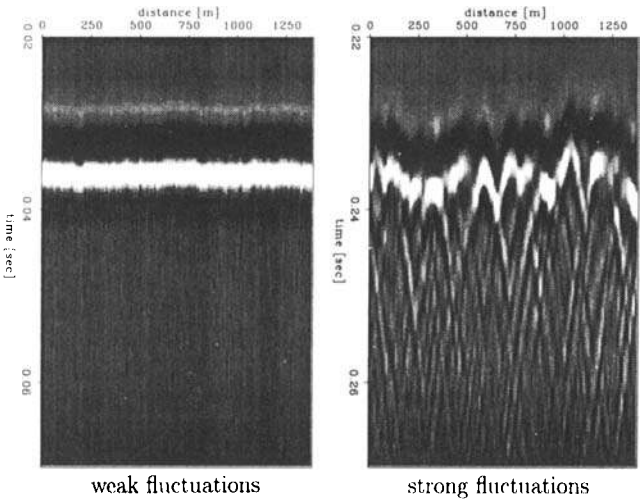

Figure 6. Shot records registered in the region of weak wavefield fluctuations (left) with $\alpha_{\langle u\rangle}L = 0.04$ and $\theta \approx 0.3$, and strong-wavefield fluctuations (right) with $\alpha_{\langle u\rangle}L = 1.24$ and $\theta \approx 3.3$. Both plots are normalized to their maximum and no time-dependent scale has been applied.

resp $\alpha_{\langle u\rangle}L = 1.24$. Each plot is normalized to its maximum and no time-dependent scale has been applied. In the weak fluctuation region the wavefront of the first arrival is distorted compared to wave propagation in a homogeneous medium. The larger the travel distance the stronger the wavefield fluctuates and the larger the portion of energy transferred to the coda. In the region of strong fluctuations it is impossible to determine for a certain trace where the first arrival ends and where the coda begins. The amplitudes of the first arrivals can have the same order of magnitude than the fluctuations several periods afterwards. Intuition already implies that determining attenuation from amplitudes in the region of strong wavefield fluctuations could be problematic. In fact as already mentioned above $\langle \ln A\rangle$ and $\ln\langle A\rangle$ tend to constants. The stronger linear events in Fig. 6, right are diffractions at near-receiver heterogeneities.

Fig. 7, left, shows the complete meanfield traces computed for different distances in one plot. The decay with travel distance, resp traveltime is obvious. Note that the smaller the travel distance, the better the spatial averaging suppresses fluctuations. Non-perfect averaging leads to a meanfield 'tail' at large distances. If we put a box-car window around the coherent arrival and centred around the expected arrival time of the centre of mass of the event for a homogeneous medium with average slowness (Fig. 7, right) we can see pulse broadening more clearly. The amplitude spectra corresponding to Fig. 7 are shown in Fig. 8 and display the expected decrease and degeneration of high-frequency components with travel distance. The roughness of the spectra in Fig. 8, left, is due to the fluctuations 'tail' remaining after stacking the traces. The spectra get smoother with recording distance because the wave arrives later and therefore the number of samples representing fluctuations decreases. For comparison the input wavelet spectrum is included in the plots (uppermost curves). The amplitude spectra of the windowed meanfield (Fig. 8, right) show the same decay and shift of the dominating frequency to lower frequencies. Now the spectra are smooth because random fluctuations caused by non-perfect averaging are largely left outside the window.

Fig. 9 shows $\ln|\langle u\rangle|$ (top, left), $\langle \ln A\rangle$ (top, right), $\ln\langle A\rangle$ (bottom, left), and $\ln\langle A^2\rangle$ (bottom, right) as function of travel-distance L and for the dominant frequency of 100 Hz. Theory is represented by solid lines [relation (A2–15) has been used for $\ln|\langle u\rangle|$, relations (22) and (36) for $\langle \ln A\rangle$ and $\ln\langle A\rangle$] and logarithms calculated from synthetic data are denoted by dots. The meanfield shows the predicted behaviour. The straight line indicates that attenuation is independent on the travel distance. Log values scatter farther away from the theoretical curve at large distances because the spatial averaging does not suppress incoherent energy sufficiently. Mean logarithm of amplitude and logarithm of mean amplitude follow closely the theory in the region of weak wavefield fluctuations (bent curve). Finally, Fig. 9, bottom right, proves that backward scattering could be neglected in our simulation because the total intensity registered remains approximately constant and its ln scatters near zero. The slight shift of these values in the positive direction can be explained by some reasons. The first is our normalization procedure, where all spectra were normalized by the amplitude spectrum of the meanfield obtained in homogeneous strip of the model. The small amount of backscattering makes this spectrum lower amplitude than the one of the wavefield in homogeneous medium. The second reason could be resonances in the limited model space. In any case we found this positive shift small compared with the effects under investigation. The subsequent Figs 10 to 14 are similar to Fig. 9 but have been computed for frequencies of 120 Hz, 140 Hz, 160 Hz, 180 Hz and 200 Hz. Attenuation grows with frequency as predicted by the theory. Figs 10 to 14 demonstrate that the region of weak wavefield fluctuations is reduced in size with frequency and therefore compared to Fig. 9. In the growing region of strong wavefield fluctuations the values scatter near the constants $-0.25\ln 2 \approx -0.173$ for the mean logarithm of

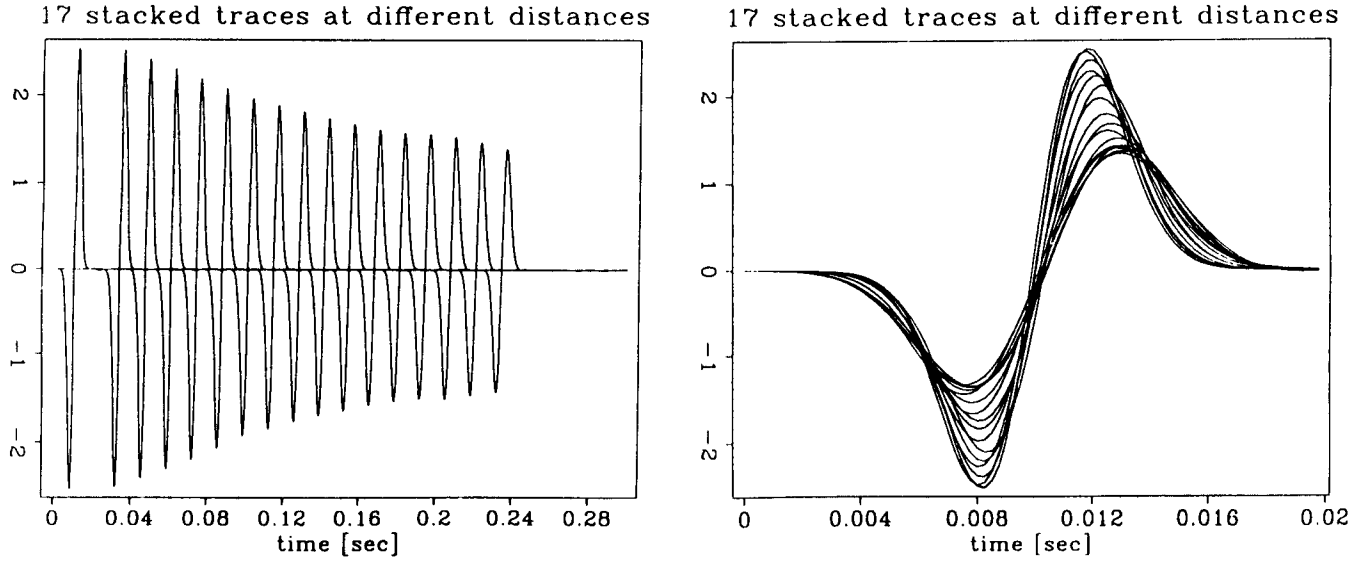

Figure 7. Meanfield traces of the wavefield recorded at different travel distances in a medium with 3 per cent velocity perturbation. The plots show 17 traces above each other. The complete meanfield traces (left) show the decrease with traveltime, resp travel distance. Meanfield has been windowed by a rectangular window centred around the arrival travelling with average slowness (right).

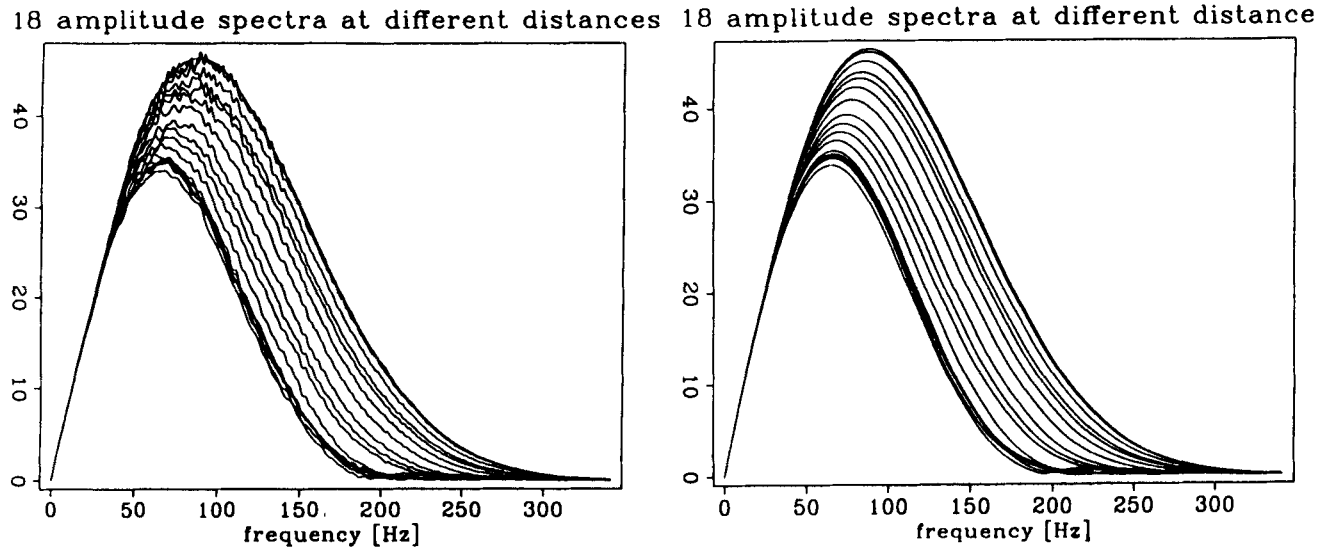

Figure 8. Meanfield amplitude spectra computed at different travel distances. The spectra have been computed from the data in Fig. 7. Spectra of the complete traces (left) are rough because the meanfield coda is not zero, i.e. spatial averaging is not perfect. Amplitude spectra of the windowed traces are smooth. The decrease and shift to lower frequencies reflects the behaviour of meanfield amplitudes. For reference the amplitude spectrum of the input wavelet is also shown.

amplitude, and resp $-0.125 \ln 2 \approx -0.087$ for the logarithm of the mean amplitude as expected from the theory.

In summary, we find good agreement between the theory and the numerical simulations. Small deviations from theory in Figs 7 to 14 can be explained by non-perfect averaging and therefore can be reduced by improved spatial averaging or by ensemble averaging. Our results not only prove that our theory works but also that high-order finite difference operators can be applied to model random-media wave propagation highly accurately.

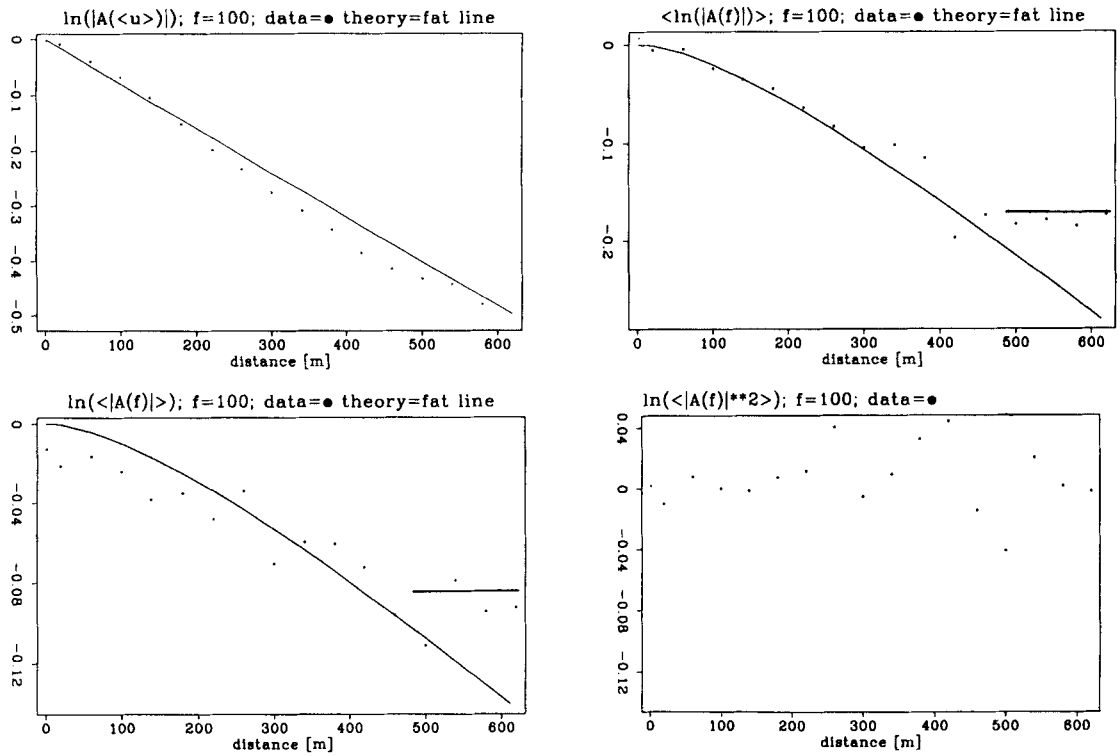

Figure 9. $\ln |\langle u \rangle|$ (top, left), $\langle \ln A \rangle$ (top, right), $\ln \langle A \rangle$ (bottom, left), and $\ln \langle A^2 \rangle$ (bottom, right) for the dominant frequency of 100 Hz. Points denote the numerical experiment, solid lines denote theory. The bent curve in the Figures of $\langle \ln A \rangle$ and $\ln \langle A \rangle$ refers to the weak fluctuation region and the horizontal line to the strong fluctuation region.

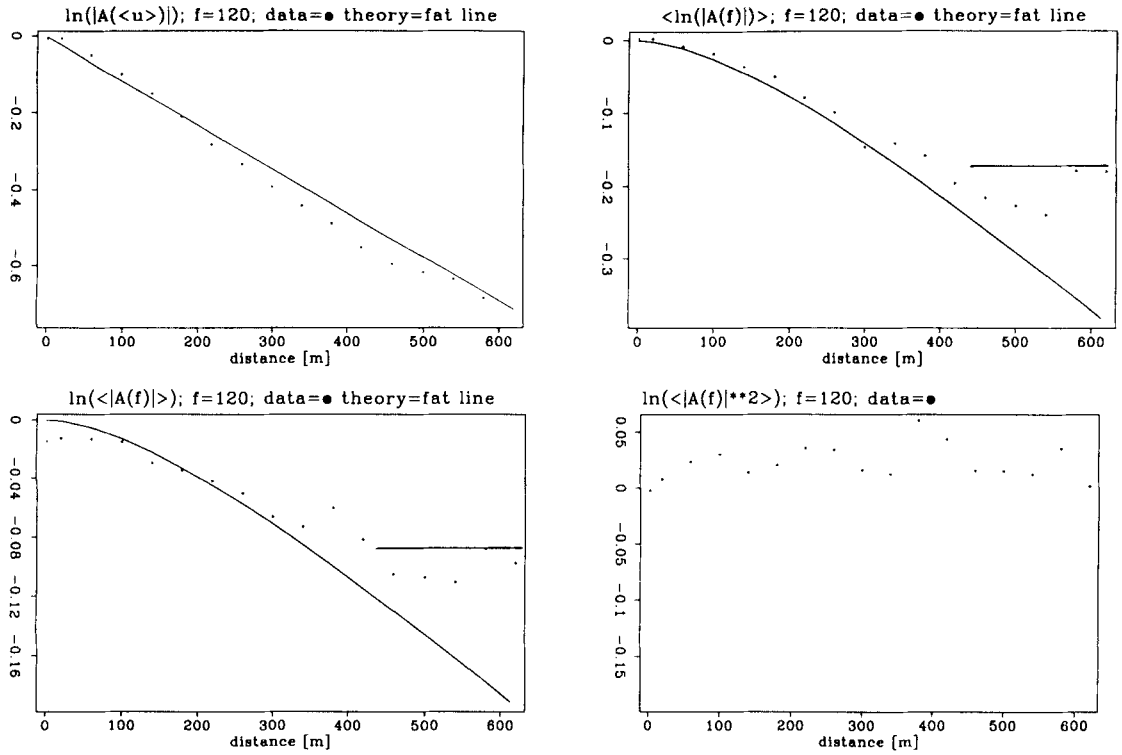

Figure 10. The same as Fig. 9, but for the frequency of 120 Hz.

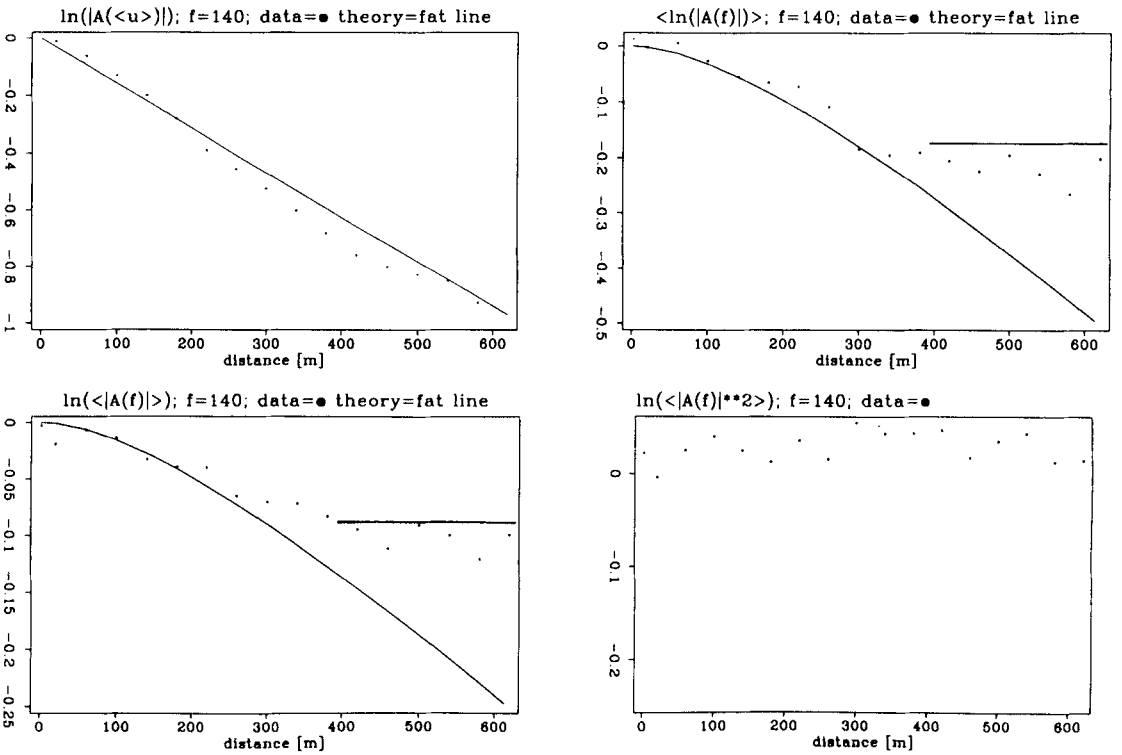

Figure 11. The same as Fig. 9, but for the frequency of 140 Hz.

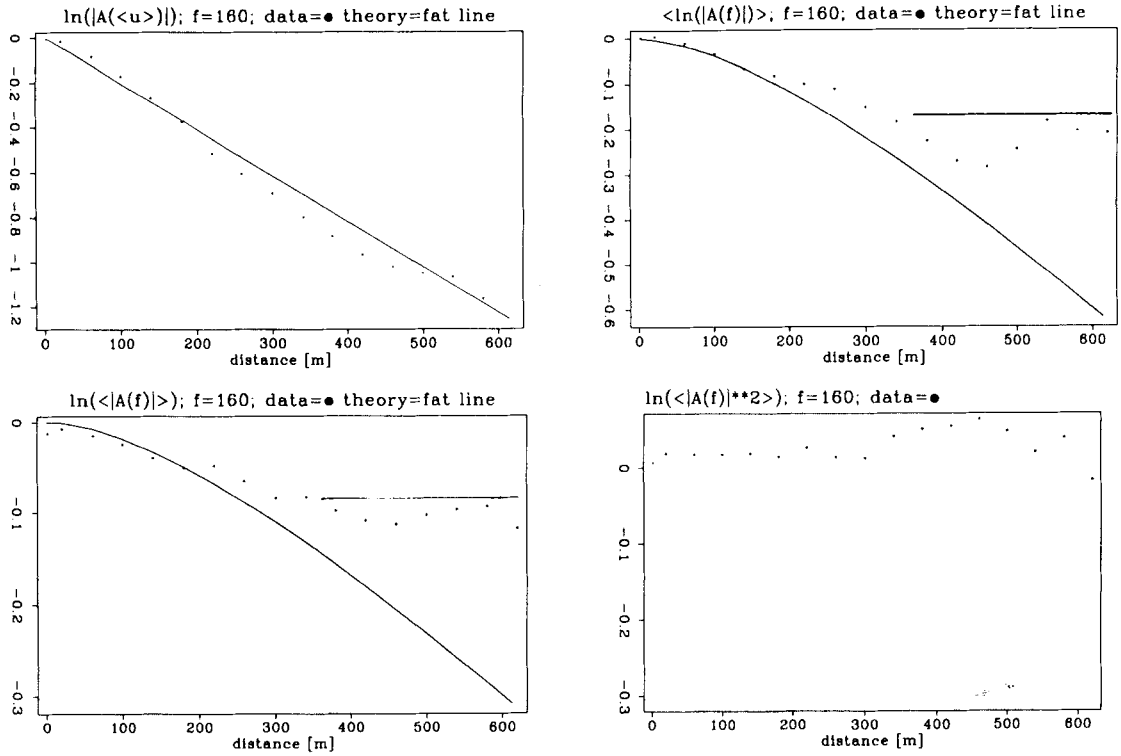

Figure 12. The same as Fig. 9, but for the frequency of 160 Hz.

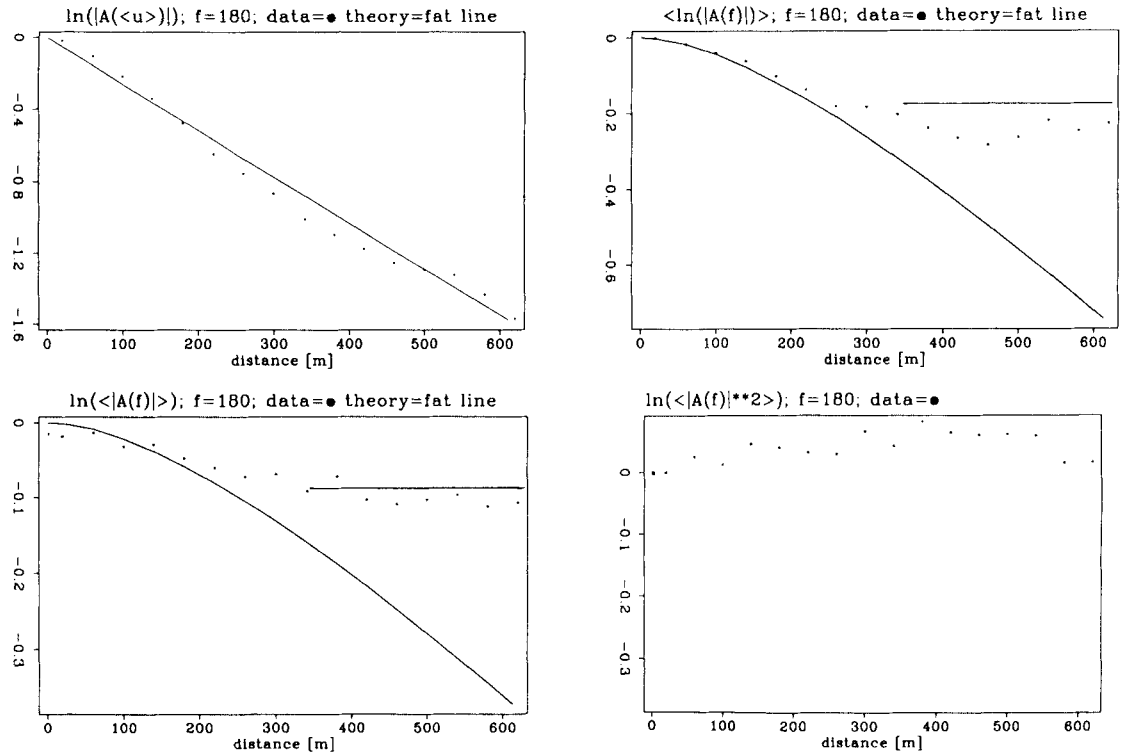

Figure 13. The same as Fig. 9, but for the frequency of 180 Hz.

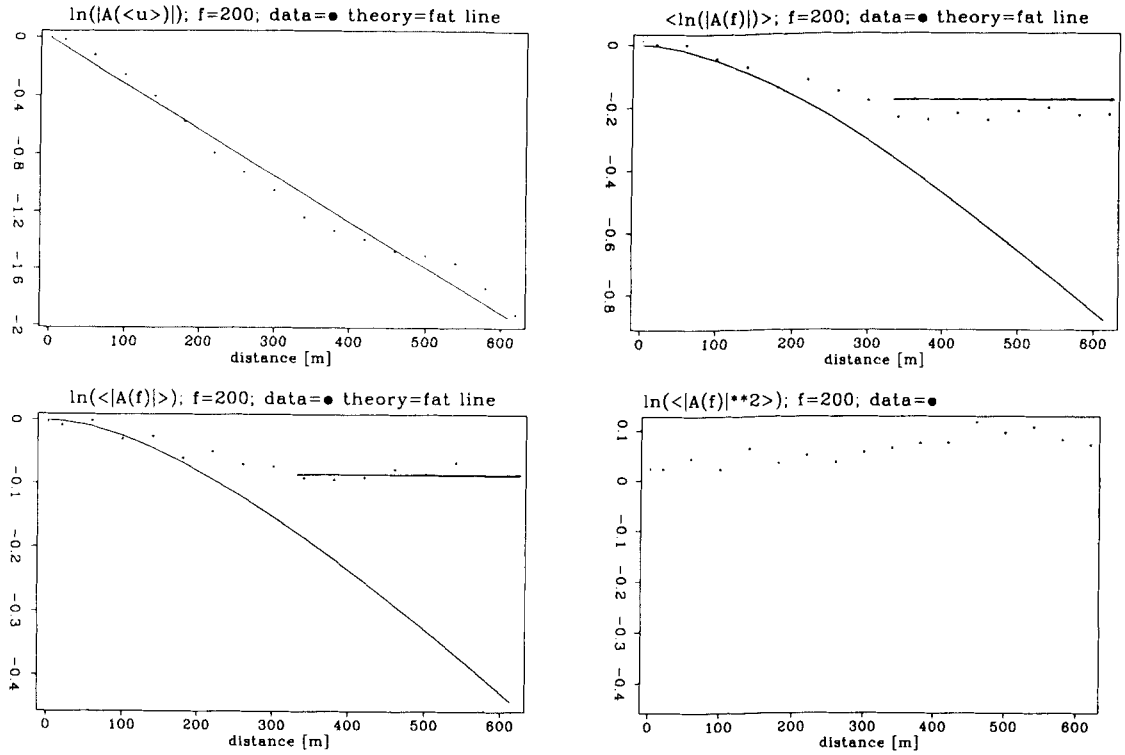

Figure 14. The same as Fig. 9, but for the frequency of 200 Hz.

DISCUSSION

In this paragraph we discuss usefulness and restrictions of our results and consider some perspectives and open questions.

The main conclusion of our theoretical and numerical consideration is that if scattering plays a noticeable role compared with absorption we cannot apply a linear regression to obtain attenuation estimates from the travel-distance dependencies of logarithms of amplitude spectra. We propose a theory which could be a base for studying scattering properties of heterogeneous media from these dependencies.

First we have to make the following remark. Our analysis was performed for media without any absorption and with the negligible backscattering. This leads to the independence of total intensity I_t on travel distance. This means that the mean energy is being conserved. Therefore, the dependence of the logarithms of amplitude spectra on the travel distance does not describe the attenuation of the mean energy but the average decrease of amplitude spectra because of increasing energy fluctuations. This increase cannot be unlimited and in the strong fluctuation region a saturation of the energy fluctuations occurs which yields constant logarithms of amplitude spectra.

Now let us discuss the restrictions of the presented concepts.

Impulse wavefield

The theory presented here considers only propagation of harmonic wavefields. Therefore, the generalization to impulse wavefields is an open and practically relevant problem. Intuitively it is clear that the estimations of the scattering attenuation obtained from logarithms of amplitude spectra will depend on the length and kind of the window applied to extract the direct arrivals. The larger the window the more samples of the fluctuating field will be analysed and in the limit of infinite window the results will tend to the results for harmonical wavefields. We assumed that inhomogeneities are not too small and we neglected the backscattering. This means that wavefield fluctuations are caused mainly by scattering within the volume of the medium between source and receiver. This volume additionally is limited by the small scattering angle. Windowing data leads to a similar restriction of the scattering volume. Therefore, we can expect that our theoretical results describe estimations obtained only from direct arrivals too, at least qualitatively. In order to demonstrate this we repeated the processing described above but did this after applying a box-car window around the direct arrivals having 1.5 times the length of the input wavelet. We find good agreement with the theory for the harmonic wavefield in the weak fluctuation region (Figs 15–17). The strong fluctuation region now begins later (compare Figs 9, 12, 14 and Figs 15–17) and probably the level of saturation changed.

The second aspect of windowing is the window shape. The choice of a window always has to compromise between the amount of variance and bias introduced. We came to the conclusion that the choice of a window function is less important where many spectra or traces can be averaged to perform the spectral estimation because averaging smooths and bias partly averages away. In practice, data volumes

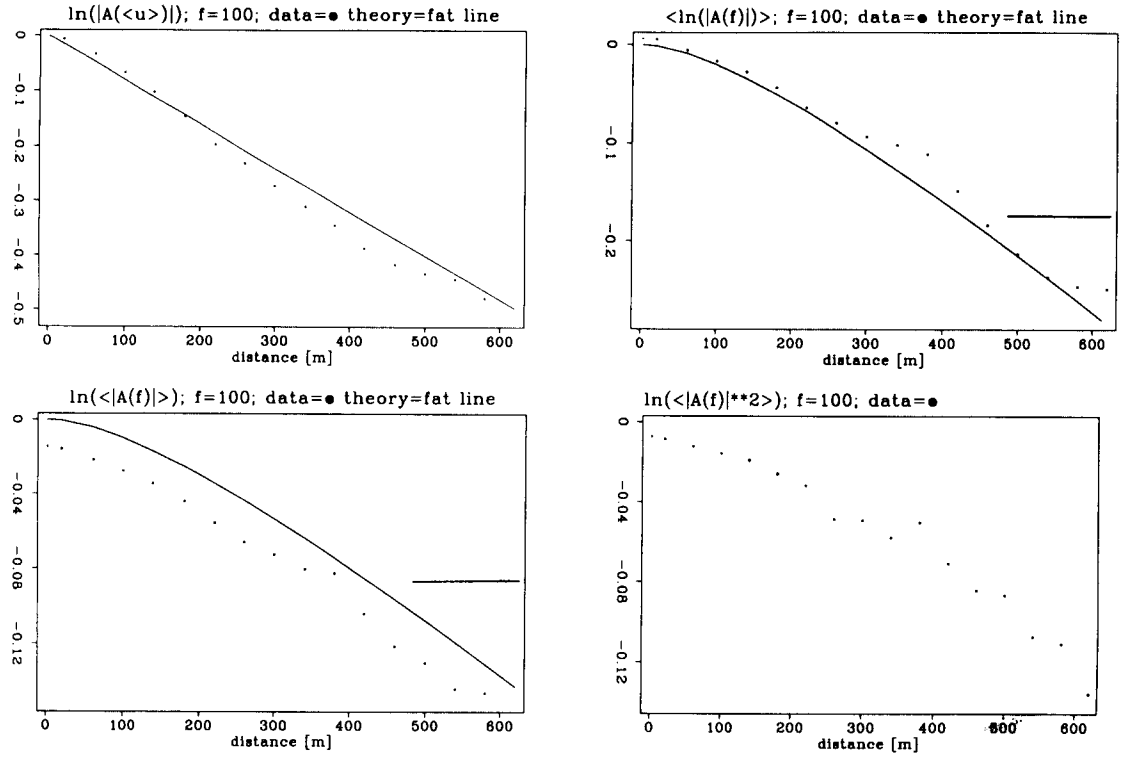

Figure 15. The same as Fig. 9, but the processing has been performed after windowing around direct arrivals. The frequency is 100 Hz.

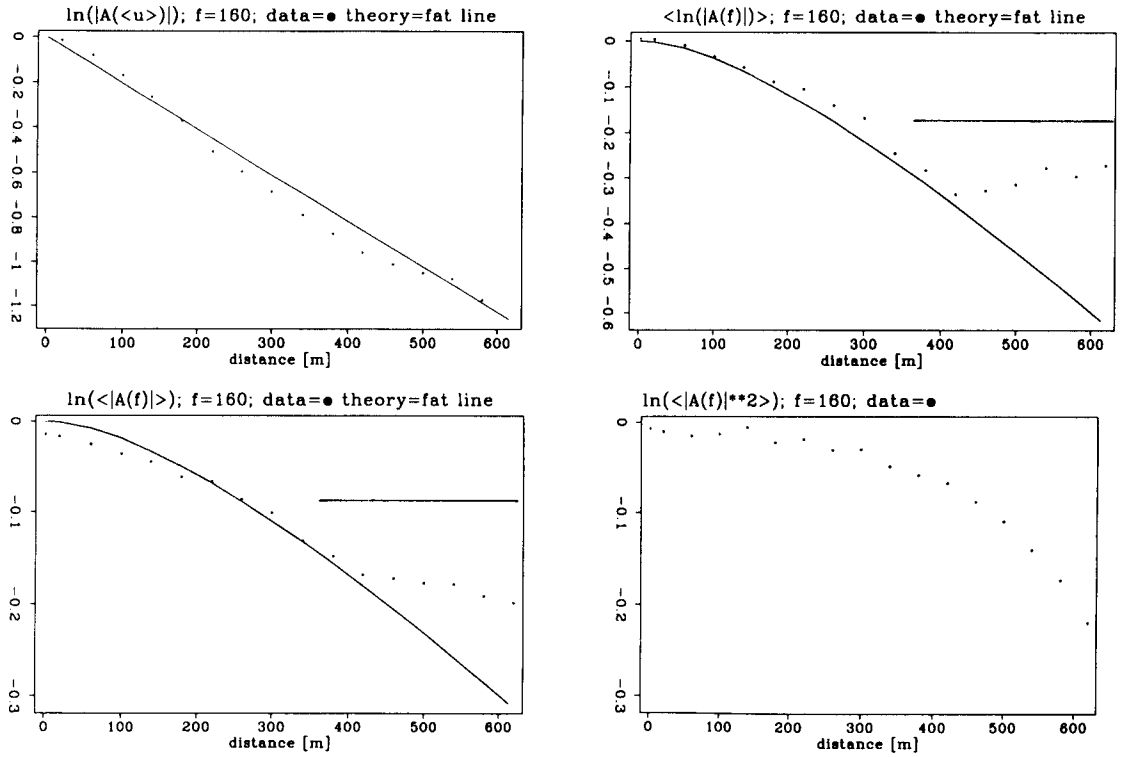

Figure 16. The same as Fig. 15, but for the frequency of 160 Hz.

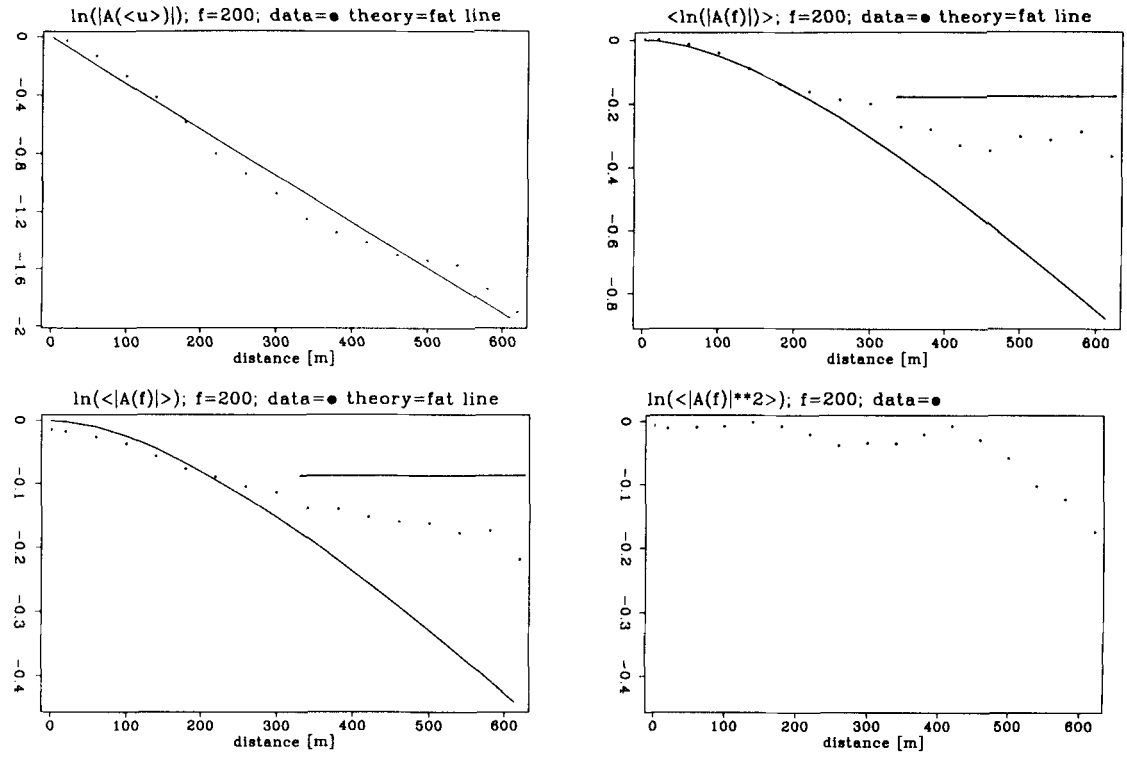

Figure 17. The same as Fig. 15, but for the frequency of 200 Hz.

often do not allow sufficient averaging. In that case the shape of the window is an important subject. But it will not be considered here.

Point source

Another principal limitation of the presented theory is that it has been developed for an incident plane wave. At least partially this theory can be generalized for a point source in a random medium. Relations (16), (17) and (18) are valid for the case of spherical waves, too. The relations for the amplitude level variance can be obtained in the same way as described in Appendix 1, and also in Ishimaru (1978). Particularly, for the 2-D case, we obtain an equation which is similar to the corresponding equation for a plane wave:

$$\sigma^2_{\chi,\text{point}} \approx 4k^2\pi \int_0^L d\eta \int_0^\infty d\xi \sin^2\left[\frac{\xi^2}{2kL}\eta(L-\eta)\right]\Phi_n^{2\text{-D}}(\xi). \quad (47)$$

This relation together with the relations (16) and (17) yields a generalization of the presented theory to the case of a point source and for the weak fluctuation region. But this description is not complete because we still need a theory for the total intensity in the presence of large inhomogeneities. Relation (18) represents a value, which is measurable and which is independent of the total intensity, i.e. it is described by $\sigma^2_{\chi,\text{point}}$ only.

Relation (47) shows a complicated dependence of $\sigma^2_{\chi,\text{point}}$ on travel-distance L. Again we cannot apply a linear regression to obtain attenuation estimates from the dependence of the logarithm of the amplitude spectra on the travel distance (even after correction for geometrical spreading). Of course, the results for a plane wave can be used directly for large travel distances where we can approximate the spherical wave by a plane wave.

Frequency domain

The next limitation of the presented theory we want to discuss is the restriction on the frequency range. The limitation $a \gtrsim \lambda$ can be expressed by the dimensionless wavenumber $ka \gtrsim 2\pi$. No upper frequency limit exists. This follows from the theoretical results for the correlation function of the phase where we obtained the geometrical optics approximation as the high frequency limit. In our experiments we investigated the range $1 \leq ka \leq 12$ and found good agreement between finite difference simulations and the theory. Smaller ka values, i.e. longer wavelengths or weaker scattering, are more difficult to investigate numerically at least if the region of strong fluctuations is of interest because spatial averaging is less effective at large wavelengths and sufficient ensemble averaging would require much more computational efforts. The low-frequency limit of our theory is required to exclude backscattering. The theory is based on the parabolic approximation of the wave equation and therefore demands strong forward scattering. The generalization to small inhomogeneities is an open problem.

Other limitations

In our theory we also assume an isotropic autocorrelation function of the medium fluctuations, i.e. of n_1. In an additional experiment (no pictures shown) we choose the correlation length parallel to the wavefront of the plane

wave a_x unchanged (20 m) but increased the correlation length perpendicular a_z to 50 m. Compared to the isotropic medium ($a_x = a_z = 20$ m) the transition from the weak to the strong-fluctuation regions occurs at shorter travel distances and smaller frequencies indicating stronger scattering. The higher the frequency the stronger predominates small-angle scattering and the better is the fit to the theory for the isotropic medium. The wave interacts practically only with the scattering cross-section parallel to the wavefront which defines an 'effective' correlation length.

Our theory also demands the velocity perturbations of the random medium to be small. We found good agreement between simulations and theory in the range $1\% \leq \sqrt{\sigma_n^2} \leq 10\%$. Smaller perturbations pose no problem but the larger σ_n^2 the stronger scattering and the less effective is averaging. Again we meet practical limits of the computer simulation.

Application to inverse problems

The main aim of our paper has been an analysis of the forward problem. Let us discuss now some possibilities to apply the presented theory to inverse problems.

Using wavefield-amplitude fluctuations for inverse problems is often obscured by the coupling effect originating in a small region around a source or a receiver. In more or less stationary media we can hope that the coupling does not systematically depend on travel distance. Our results give the systematic relationships between the logarithms of wavefield amplitudes and travel distance. Therefore, the curves of the logarithms of amplitudes versus travel distance (in a weak fluctuation region) are more or less free of the influence of the coupling effect. These curves are Fourier-type integrals of the media-fluctuation spectra and therefore they can be inverted.

As noted before it is not adequate to apply linear regression to the travel distance dependencies of the logarithms of amplitudes. But what could be approximated by a straight line is the sum $-\langle \ln A \rangle + \sigma_s^2$ [see (21) and (27)]. In the absence of absorption the slope of this straight line will be equivalent to $2\alpha_s$ and in presence of absorption it will be $\alpha_a + 2\alpha_s$. The slope of $\ln |\langle u \rangle|$ plotted as a function of travel distance is $\alpha_a + \alpha_s$. Subtraction yields α_s, i.e. allows us to separate absorption and scattering effects. By studying phase fluctuations, the travel distance dependence of the logarithms of wavefield amplitudes and of meanfield amplitudes, and the linear regression described above, we can take into account the contributions of scattering and absorption in different ways. This enables us to estimate the strength of scattering and absorption separately.

CONCLUSIONS

If scattering plays a noticeable role compared to absorption we cannot apply a linear regression to obtain attenuation estimates from the travel-distance dependencies of the logarithms of the amplitude spectra. Our results describe these estimates and can be a base for studying the scattering properties of the earth using these dependencies and (or) traveltime fluctuations. Different scattering attenuation estimates are obtained by averaging different wavefield attributes. α_A and $\alpha_{\ln A}$ depend on travel distance, while $\alpha_{\langle u \rangle}$ does not. The behaviour of the logarithm of mean amplitude and the mean logarithm of amplitude are completely different in the weak and strong-fluctuation regions. They depend non-linearly on travel distance if the wavefield fluctuations are small and can be tied with the logarithm of the meanfield. The averages $\langle \ln A \rangle$ and $\ln \langle A \rangle$ differ approximately by a factor two. In the region of strong wavefield fluctuations they tend to the constants -0.173, resp -0.087. Decrease in the total intensity can be attributed to absorption as long as the weak scattering approximation holds and backscattering can be neglected. The slope of $\langle \ln A \rangle$ and $\ln \langle A \rangle$ plotted versus travel distance will be the absorption coefficient α_a in the region of strong wavefield fluctuations.

ACKNOWLEDGMENTS

We thank C. Kerner for helping us to prepare the random models. Discussions with P. Harris and P. Williamson improved the paper. Research was funded in part by the Commission of the European Communities in the framework of the JOULE programme, subprogramme Energy from Fossil Sources: Hydrocarbons, project JOUF 0048C; and by the Alexander von Humboldt Foundation.

REFERENCES

Aki, K. 1980. Scattering and attenuation of shear waves in the lithosphere, *J. geophys. Res.*, **85,** 6496–6504.

Aki, K. & Chouet, B., 1975. Origin of coda waves: source, attenuation and scattering effects, *J. geophys. Res.*, **80,** 3322–3342.

Davies, J. H., Gudmundsson, O. & Clayton, R. W., 1992. Spectra of mantle shear wave velocity structure, *Geophys. J. Int.*, **108,** 865–882.

Fayzullin, I. S. & Shapiro, S. A., 1988. Scattering and the dependency of seismic wave attenuation on the length of the observation base, I: elements of a theory, *Izv., Earth Phys.*, **24,** 103–110.

Frankel, A. & Clayton, R. W., 1986. Finite difference simulations of seismic scattering: implications for the propagation of short-period seismic waves in the crust and models of crustal heterogeneity, *J. geophys. Res.*, **91,** 6465–6489.

Gibson, B. S. & Levander, A. R., 1990. Apparent layering in common-midpoint stacked images of two-dimensionally heterogeneous targets, *Geophysics,* **55,** 1466–1477.

Gudmundsson, O., Davies, J. H. & Clayton, R. W., 1990. Stochastic analysis of global traveltime time data: mantle heterogeneity and random errors in the ISC data, *Geophys. J. Int.*, **102,** 25–43.

Hudson, J. A., 1990. Attenuation due to second-order scattering in material containing cracks, *Geophys. J. Int.*, **102,** 485–490.

Ishimaru, A., 1978. *Wave propagation and scattering in random media*, Vols 1 and 2, Academic Press, New York.

Jannaud, L. R., Adler, P. M. & Jacquin, C. G., 1991. Spectral analysis and inversion of codas, *J. geophys. Res.*, **96,** 18215–18231.

Keller, J. B., 1964. Stochastic equations and wave propagation in random media, *Proc. Symp. appl. Math.*, **16,** 145–170.

Kneib, G. & Kerner, C., 1992. Accurate and efficient seismic modeling in random media, *Geophysics,* **58,** 576–588.

Morse, P. M. & Feshbach, H., 1953. *Methods of theoretical physics,* McGraw-Hill, New York.

Müller, G., Roth, M. & Korn, M., 1992. Seismic-wave traveltimes in random media, *Geophys. J. Int.*, **110,** 29–41.

Pujol, J. & Smithson, S., 1991. Seismic wave attenuation in volcanic rocks from VSP expriments, *Geophysics,* **56,** 1441–1455.

Rytov, S. M., Kravtsov, Y. A. & Tatarskii, V. I., 1987. *Principles of statistical radiophysics*, Springer, New York.

Sato, H., 1982. Amplitude attenuation of impulsive plane waves in random media based on traveltime corrected mean wave formalism, *J. Acoust. Soc. Am.*, **71**, 599–564.

Wu, R.-S., 1982a. Mean field attenuation and amplitude attenuation due to wave scattering. *Wave Motion*, **4**, 305–316.

Wu, R.-S., 1982b. Attenuation of short period seismic waves due to scattering, *Geophys. Res. Lett.*, **9**, 9–12.

Wu, R.-S., 1985. Multiple scattering and energy transfer of seismic waves—separation of scattering effect from intrinsic attenuation—I. Theoretical modelling, *Geophys. J. R. astr. Soc.*, **82**, 57–80.

APPENDIX 1

Derivation of amplitude level and phase correlation functions

In this appendix we derive the dependencies of the amplitude level and phase-fluctuations correlation functions on frequency, travel distance, and the statistical medium properties. Taking the amplitude correlation function at zero lag yields the variance which can be substituted into (21) and (22) to obtain $\langle \ln A \rangle$ and $\ln \langle A \rangle$. We derive these relations for 2-D wave propagation (these results are new to our knowledge) and compare them in the main text to Ishimaru (1978) who has already presented most of the analogous formulae for the 3-D case.

Following the derivation of Ishimaru (1978) for the 3-D case, we study the amplitude variance for harmonic plane waves in the Rytov approximation, which gives for

$$u(\mathbf{r}) = u_0(\mathbf{r}) \exp[\psi(\mathbf{r})]; \qquad \psi \equiv \chi + is \tag{A1-1}$$

the first iteration

$$\psi(\mathbf{r}) \approx \psi_1(\mathbf{r}) \equiv 2k^2 \int_{V'} G(\mathbf{r}-\mathbf{r}') n_1(\mathbf{r}') \frac{u_0(\mathbf{r}')}{u_0(\mathbf{r})} dV'. \tag{A1-2}$$

Here k is the wavenumber, G is the Green's function for a n-D medium, and V' is the volume containing scatterers. In the 2-D case the Green's function of harmonic waves is given by (A2-2). For a large volume V' one can expect that the main contribution in ψ is given by inhomogeneities far away from the receiver point $\mathbf{r}$. We can use the far-field approximation of the Green's function (A2-3). Our next assumption is that the size of inhomogeneities a (or the correlation radius) is not much smaller than the wavelength: $\lambda \lesssim a$. Moreover, if there exist inhomogeneities of different scale lengths, large inhomogeneities will give the main contribution (provided that they are not too few). These assumptions permit us to neglect backscattering, i.e. in (A1-2) the integration can be limited to the interval $0 \le x \le L$. Furthermore, in the Green's function we can assume $|z - z'| \ll |x - x'|$ because scattering is confined with an angle of order λ/a in the forward direction. This yields the following approximation for the Green's function:

$$G(\mathbf{r}-\mathbf{r}') \approx \frac{i}{4} e^{i(-\pi/4)} \left(\frac{2}{\pi k |x-x'|} \right)^{1/2} e^{ik\left[x-x' + \frac{(z-z')^2}{2(x-x')}\right]}. \tag{A1-3}$$

Next we introduce the representation of the random medium fluctuation $n_1(\mathbf{r})$ in the space-wavenumber domain

$$n_1(x, z) = \int e^{i\xi z} \, dv(x, \xi). \tag{A1-4}$$

Integration in (A1-2) over z' gives

$$\psi_1(L, z) = ik \int_{-\infty}^{\infty} dv(x', \xi) \int_0^L dx' e^{i\xi z} e^{-i\frac{\xi^2}{2k}(L-x')}. \tag{A1-5}$$

The complex conjugate function ψ^* reads

$$\psi_1^*(L, z) = -ik \int_{-\infty}^{\infty} dv(x', \xi) \int_0^L dx' e^{i\xi z} e^{i\frac{\xi^2}{2k}(L-x')}. \tag{A1-6}$$

Here the identity $dv(x', \xi) = dv^*(x', -\xi)$ and the substitution $\xi \to -\xi$ were used. With (A1-5) and (A1-6) we obtain for χ:

$$\begin{aligned} \chi(L, z) &= \tfrac{1}{2}[\psi_1(L, z) + \psi_1^*(L, z)] \\ &= k \int_{-\infty}^{\infty} dv(x', \xi) \int_0^L dx' e^{i\xi z} \sin\left[\frac{\xi^2}{2k}(L-x')\right]. \end{aligned} \tag{A1-7}$$

The spatial-amplitude level-correlation function $B_\chi = \langle \chi(L, z_1) \chi^*(L, z_2) \rangle$ reads

$$\begin{aligned} B_\chi(\Delta z) = k^2 \int_{-\infty}^{\infty} d\xi \int_0^L dx' \int_0^L dx'' e^{i\xi \Delta z} \sin\left[\frac{\xi^2}{2k}(L-x')\right] \\ \times \sin\left[\frac{\xi^2}{2k}(L-x'')\right] F(|\Delta x|, \xi), \end{aligned} \tag{A1-8}$$

where $\Delta z = z_1 - z_2$; $\Delta x = x' - x''$, $\langle dv(x', \xi') \, dv(x'', \xi'') \rangle = F(|\Delta x|, \xi') \delta(\xi' - \xi'') \, d\xi'$, and

$$F(|\Delta x|, \xi) = [1/(2\pi)] \int_{-\infty}^{\infty} \langle n_1(x, z) n_1(x + \Delta x, z + \Delta z) \rangle e^{i\xi \Delta z} \, d\Delta z.$$

We introduce the new centre of mass coordinates $\eta = 0.5(x' + x'')$ and the difference coordinates $\Delta x = (x' - x'')$ and perform the integration over Δx from $-\infty$ to ∞. The latter is admissible because $F(|\Delta x|)$ differs from 0 noticeably only within the correlation distance, i.e. for $\Delta x \lesssim a$. We finally use

$$\sin[(\xi^2/(2k))(L - x')] \approx \sin[(\xi^2/(2k))(L - \eta)]$$

and obtain from (A1-8)

$$B_\chi(\Delta z) = 2k^2 \pi \int_0^L d\eta \int_{-\infty}^{\infty} d\xi e^{i\xi \Delta z} \sin^2\left[\frac{\xi^2}{2k}(L-\eta)\right] \Phi_n^{2\text{-D}}(\xi), \tag{A1-9}$$

where $\Phi_n^{2\text{-D}}$ is the fluctuation spectrum of the refractive index n_1 determined in (A2-7). Finally, the integration over η gives the correlation function of the amplitude level.

$$B_\chi(\Delta z) = 2k^2 \pi L \int_0^{\infty} \cos(\xi \Delta z) \left(1 - \frac{\sin(\xi^2 L/k)}{\xi^2 L/k}\right) \Phi_n^{2\text{-D}}(\xi) \, d\xi. \tag{A1-10}$$

By the analogous calculation we obtain the phase correlation function

$$B_s(\Delta z) = 2k^2 \pi L \int_0^{\infty} \cos(\xi \Delta z) \left(1 + \frac{\sin(\xi^2 L/k)}{\xi^2 L/k}\right) \Phi_n^{2\text{-D}}(\xi) \, d\xi. \tag{A1-11}$$

Substituting $B_s(\Delta z) = B_T(\Delta z)\omega^2$ only changes the factor in front of the integral and yields traveltime fluctuations. The analytical formulae (A1-10) and (A1-11) describe amplitude level and phase, respectively traveltime fluctuations of a random field in the region of weak wavefield fluctuations in 2-D media. They are very useful in studying fluctuations of χ, s and traveltime.

APPENDIX 2

Meanfield

Here we derive the scattering cross-section Σ of a unit volume in a 2-D random medium, and from that obtain the scattering coefficient of the meanfield. Most of the presented results are used in the main part of the text and, therefore, are necessary for consideration. The formula for the scattering coefficient of the meanfield in 2-D exponential random media is new to our knowledge and it will be used in the numerical experiment.

The scattering cross-section is the ratio of the power flux scattered by the unit volume in all directions to the incident power flux per unit surface. Note that the scattering cross-section is a far-field characteristic of scattering. In order to find the scattering cross-section we write the scattered field u^s as

$$u^s(\mathbf{r}) = k^2 \int_{V'} G(\mathbf{r}-\mathbf{r}') 2n_1(\mathbf{r}') u(\mathbf{r}')\, dV' \qquad \text{(A2-1)}$$

assuming the secondary sources are the inhomogeneities of the medium confined by the volume V'. Here G is the Green's function and k is a wavenumber in the homogeneous background medium. The Green's function of harmonical waves in two dimensions reads (Morse & Feshbach 1953)

$$G(\mathbf{r}-\mathbf{r}') = \frac{i}{4} H_0^{(1)}(kR), \qquad \text{(A2-2)}$$

where $R = |\mathbf{r}-\mathbf{r}'|$ and $\mathbf{r}'$ is the radius vector of the source. $H_0^{(1)}$ is a Hankel function of the first kind. In the far field of the scattering volume we can use the far-field approximation of the Green's function

$$G(R) \approx \frac{i}{4}\left(\frac{2}{\pi k R}\right)^{1/2} e^{i(kR - \pi/4)}. \qquad \text{(A2-3)}$$

Supposing that the scattering volume is located at the origin we can now write the far-field approximation of the scattered field

$$u^s(\mathbf{r}) = f(\mathbf{j},\mathbf{i})\left(\frac{1}{r}\right)^{1/2} e^{ikr}, \qquad \text{(A2-4)}$$

where the unit vector $\mathbf{j}$ describes the direction of scattering; the unit vector $\mathbf{i}$ describes the propagation direction of the incident plane wave. $f(\mathbf{j},\mathbf{i})$ is the scattering amplitude

$$f(\mathbf{j},\mathbf{i}) = \frac{ik^2}{4}\left(\frac{2}{\pi k}\right)^{1/2} e^{-i\pi/4} \int_{V'} 2n_1(\mathbf{r}') e^{-ik\mathbf{j}\cdot\mathbf{r}'} u(\mathbf{r}')\, dV'. \qquad \text{(A2-5)}$$

In the Born approximation, which is valid for low-contrast inhomogeneities (weak scattering) we can substitute in this integral equation the incident plane wave $\exp(ik\mathbf{i}\cdot\mathbf{r}')$ instead of $u(\mathbf{r}')$ (Ishimaru 1978). Using this substitution we obtain the differential scattering cross-section of the unit scattering volume

$$\Sigma(\mathbf{j},\mathbf{i}) \equiv \frac{1}{V'}\langle f(\mathbf{j},\mathbf{i}) f^*(\mathbf{j},\mathbf{i})\rangle \approx 2\pi k^3 \Phi_n^{2\text{-D}}(\mathbf{k}_s), \qquad \text{(A2-6)}$$

where $\mathbf{k}_s = k(\mathbf{i}-\mathbf{j})$ and

$$\Phi_n^{2\text{-D}}(\mathbf{k}) = \frac{1}{(2\pi)^2}\int_{-\infty}^{\infty} B_n(\Delta\mathbf{r}) e^{ik\Delta\mathbf{r}} d^2\Delta\mathbf{r} \qquad \text{(A2-7)}$$

is the fluctuation spectrum, i.e. the 2-D Fourier transform of the medium-correlation function

$$B_n(\Delta\mathbf{r}) = \langle n_1(\mathbf{r}) n_1(\mathbf{r}+\Delta\mathbf{r})\rangle. \qquad \text{(A2-8)}$$

The differential scattering cross-section is defined as the ratio of the power flux scattered by a unit volume in a given direction to the incident power flux per unit surface. Integration over all directions gives the total scattering cross-section for an isotropic random medium

$$\Sigma = 4\pi k^3 \int_0^{\pi} \Phi_n^{2\text{-D}}(k_s)\, d\vartheta, \qquad \text{(A2-9)}$$

where ϑ is the angle between the vectors $\mathbf{i}$ and $\mathbf{j}$ and $k_s = 2k\sin(\vartheta/2)$. With an isotropic correlation function B_n it follows that

$$\Phi_n^{2\text{-D}}(k_s) = \frac{1}{2\pi}\int_0^{\infty} B_n(r) J_0(k_s r) r\, dr. \qquad \text{(A2-10)}$$

Here J_0 is the Bessel function of the first kind. Using the variable k_s instead of ϑ we can rewrite the relation for Σ as

$$\Sigma = 4\pi k^2 \int_0^{2k} \left(1 - \frac{k_s^2}{4k^2}\right)^{-1/2} \Phi_n^{2\text{-D}}(k_s)\, dk_s. \qquad \text{(A2-11)}$$

The corresponding relations for the 3-D case are

$$\Sigma = (2\pi)^2 k^2 \int_0^{2k} k_s \Phi_n^{3\text{-D}}(k_s)\, dk_s, \qquad \text{(A2-12)}$$

and

$$\Phi_n^{3\text{-D}}(k_s) = \frac{2}{(2\pi)^2}\int_0^{\infty} B_n(r)\frac{\sin(k_s r)}{k_s} r\, dr. \qquad \text{(A2-13)}$$

The attenuation of the meanfield due to scattering is described by the scattering coefficient α_s. In our single-scattering approximation

$$\alpha_s = 0.5\Sigma. \qquad \text{(A2-14)}$$

In 2-D finite-difference modelling we use an exponential random medium with isotropic correlation function $B_n = \sigma_n^2 \exp(-\Delta r/a)$, where $\Delta r = (\Delta x^2 + \Delta z^2)^{0.5}$. Substituting that into eqs (A2-10) and (A2-9) we have for the meanfield scattering coefficient:

$$\alpha_s = 2k^3 a^2 \sigma_n^2 \frac{1}{\sqrt{1+4k^2a^2}} E\left(\frac{2ka}{\sqrt{1+4k^2a^2}}, \pi/2\right), \qquad \text{(A2-15)}$$

where $E(x, \pi/2)$ is the complete elliptic integral of the second kind and has been tabulated. Note that the meanfield scattering coefficient does not depend on travel distance.

For inhomogeneities small compared to the wavelength we have in two dimensions $\alpha \propto k^3$. This is Raleigh scattering for which, in the 3-D case, $\alpha \propto k^4$ is typical. In the case of large inhomogeneities the fluctuation spectrum differs from 0 noticeably only for $k_s < 2\pi/a$ and this leads to

$$\alpha_s \approx 2\pi k^2 \int_0^{\infty} \Phi_n^{2\text{-D}}(k_s)\, dk_s \qquad \text{(A2-16)}$$

in the 2-D case and to

$$\alpha_s \approx 2\pi^2 k^2 \int_0^{\infty} k_s \Phi_n^{3\text{-D}}(k_s)\, dk_s \qquad \text{(A2-17)}$$

in three dimensions. Therefore, the scattering coefficient of the meanfield is proportional to the square of frequency in both 2-D and 3-D provided the weak-scattering approximation holds and inhomogeneities are not small. These relations hold for the more geneal Bourret and parabolic equation approximations of multiple scattering (Rytov *et al.* 1987; Ishimaru 1978). The parabolic approximation of the wave equation neglects backscattering and corresponds to our investigation of wavefield amplitude spectra and their logarithms.